ANNUAL REVIEWS

Structural Basis of SARS-CoV-2– and SARS-CoV–Receptor Binding and Small-Molecule Blockers as Potential Therapeutics

Hariharan Sivaraman,* Shi Yin Er,* Yeu Khai Choong, Edem Gavor, and J. Sivaraman

Department of Biological Sciences, National University of Singapore, Singapore 117543; email: dbsjayar@nus.edu.sg

*These authors contributed equally to this article

ANNUAL REVIEWS CONNECT

www.annualreviews.org

- Download figures
- Navigate cited references
- Keyword search
- Explore related articles
- Share via email or social media

Keywords

receptor, S-glycoprotein, COVID-19, inhibitors, coronavirus, host–pathogen interaction

Abstract

Over the past two decades, deadly coronaviruses, with the most recent being the severe acute respiratory syndrome-related coronavirus-2 (SARS-CoV-2) 2019 pandemic, have majorly challenged public health. The path for virus invasion into humans and other hosts is mediated by host–pathogen interactions, specifically virus–receptor binding. An in-depth understanding of the virus–receptor binding mechanism is a prerequisite for the discovery of vaccines, antibodies, and small-molecule inhibitors that can interrupt this interaction and prevent or cure infection. In this review, we discuss the viral entry mechanism, the known structural aspects of virus–receptor interactions (SARS-CoV-2 S/humanACE2, SARS-CoV S/humanACE2, and MERS-CoV S/humanDPP4), the key protein domains and amino acid residues involved in binding, and the small-molecule inhibitors and other drugs that have (as of June 2020) exhibited therapeutic potential. Specifically, we review the potential clinical utility of two transmembrane serine protease 2 (TMPRSS2)-targeting protease inhibitors, nafamostat mesylate and camostat mesylate, as well as two novel potent fusion inhibitors and the repurposed Ebola drug, remdesivir, which is specific to RNA-dependent RNA polymerase, against human coronaviruses, including SARS-CoV-2.

1. CORONAVIRUS OUTBREAKS

The propensity of coronaviruses to exhibit interspecies and cross-species transmission is chiefly determined by the virus's ability to bind to the receptors of new hosts (1–4). This transmissibility has resulted in the outbreak of many zoonotic coronaviruses, such as severe acute respiratory syndrome-related coronavirus (SARS-CoV) in 2003, Middle East respiratory syndrome-related coronavirus (MERS-CoV) in 2012, and the current SARS-CoV-2 pandemic, which emerged in 2019 (5, 6). These three betacoronaviruses have caused major respiratory diseases in humans, with clinical symptoms ranging from the common cold and fever to severe lung injuries and even death. Given that there are currently no antivirals or vaccines against any of these three viruses (7), there remains an urgent need to design and test effective treatment and preventive options.

Since the emergence of SARS-CoV-2—the pathogen responsible for coronavirus disease 2019 (COVID-19)—many therapeutic regimens are being explored with the help of data garnered previously during SARS-CoV and MERS-CoV epidemics. Although vaccines remain the ultimate strategy for infection prevention, the timeline for their production may not be favorable for the COVID-19 pandemic. Alternative therapeutics such as neutralizing antibodies and small-molecule inhibitors are therefore urgently needed, and many of these have been approved for clinical trials. Repurposed drugs such as remdesivir (Gilead Sciences), developed for use against Ebola, and ritonavir and lopinavir, used against HIV, have been approved by regulatory authorities for early-phase clinical trials (8). Other early interventions, such as convalescent plasma from patients who have recovered from COVID-19 and antisera from immunized rodents, have been explored with conflicting results (2, 9, 10).

1.1. Spike Glycoprotein

Coronaviruses are positive-sense, single-stranded RNA viruses (11). Their 26–32-kb genomes encode for a polyprotein chain made up of 16 nonstructural proteins and 4 structural proteins, of which the Spike (S)-glycoprotein is the key surface protein that facilities host cellular interaction and entry (12). The S-glycoprotein comprises two proteolytically activated subunits: the S1 subunit, comprising the N-terminal domain (NTD) and a receptor binding domain (RBD), also known as the C-terminal domain (CTD), and the S2 subunit (13). The S1 subunit engages the host receptor, whereas the S2 subunit is responsible for membrane fusion (14). Crystal and cryo-electron microscopy (cryo-EM) structures of the S-glycoprotein reveal its homotrimeric conformation, with the S1 and S2 subunits present in each monomeric unit (2, 15).

1.2. Human Receptors

Exceptionally, coronaviruses from the same genus utilize different receptors and coronaviruses from different genera can utilize the same receptor (1, 16, 17). SARS-CoV, MERS-CoV, and the current SARS-CoV-2 all belong to the same genus of betacoronaviruses. SARS-CoV and SARS-CoV-2 recognize angiotensin-converting enzyme 2 (ACE2), and MERS-CoV recognizes dipeptidyl peptidase 4 (DPP4) (2, 3, 16). These factors, if extensively explored, could shed light on coronavirus pathogenesis, its cross-species potential, and the infection process and ultimately lead to ways to effectively predict zoonotic outbreaks and block future virus–receptor interactions.

1.3. Pathogen Receptor Recognition and Small-Molecule Inhibitors

Many structures of the RBD–ACE2 [Protein Data Bank Identifiers (PDB IDs): 3D0G, 6VW1] (11, 18–20) and RBD–DPP4 (PDB ID: 4L72) (16) complexes exist, thus providing a structural basis for the development of therapeutic agents (**Table 1**). Furthermore, the biochemical

Table 1 Host receptor and CoV S-glycoprotein interactions

Host protein (receptor)	Pathogen protein (CoV S)	Binding affinity (method)				Host–pathogen interaction region	Other remarks	Structure (resolution), (references)
		Host receptor construct (aa)	Pathogen CoV-S construct (aa)	Affinity (K_d)	Method			
hACE2	SARS-CoV-2 S	NTD (19–615)	RBD (319–541)	4.7 nM	SPR	Residues of hACE2 NTD interact with SARS-CoV-2 RBD and S1 subdomain.	RRAR furin cleavage site at the S1/S2 subunit. Gln493 and Leu455 of CoV-2 S RBD stabilize Lys31 in hACE2. SARS-CoV-2 RBDs have a higher affinity for hACE2 than SARS-CoV RBDs do. Antibodies target the S-glycoprotein.	PDB ID: 6M0J (X-ray 2.45 Å) (18) PDB ID: 6VW1 (X-ray 2.68 Å) (19) PDB ID: 6LZG (X-ray 2.5 Å) (2) PDB ID: 6VYB (S-glycoprotein ectodomain, open state, cryo-EM 3.2 Å) (12) PDB ID: 6VXX (S-glycoprotein, closed state, cryo-EM 2.8 Å) EMDB ID: 21457 (S-glycoprotein ectodomain, open state, cryo-EM 3.2 Å) EMDB ID: 21452 (S-glycoprotein, closed state, cryo-EM 2.8 Å)
		NTD (1–615)	Trimer (1–1208)	14.7 nM	SPR			
		NTD (1–615)	RBD-SD1 (319–591)	34.6 nM	SPR			
		NTD (19–615)	S1 (1–685)	94.6 ± 6.5 nM	SPR			
		NTD (1–615)	RBD (319–529)	44.2 nM	SPR			
		NTD (1–614)	S1 (1–685)	1.2 ± 0.1 nM	BLI			
TMPRSS2, hACE2	SARS-CoV-2 S	NA				hACE2 interacts with RBD of SARS-CoV-2.	Serine protease TMPRSS2 is used as a cofactor by SARS-CoV-2. Asn501 in CoV S RBD stabilizes Lys353 in hACE2.	(12, 33)
Human/civet hACE2	SARS-CoV S	NTD (16–615)	RBD (306–575)	31 nM	SPR	Residues in the hACE2 NTD interact with SARS-CoV RBD and S1 subdomain.	SARS-CoV S RBD mutations (Asn479Lys, Thr487Ser) reduce binding affinity to ACE2 by multiple folds. Salt bridge between Arg426 (S RBD) and Glu329 (hACE2)	PDB ID: 3D0G (X-ray 2.8 Å) (11) PDB ID: 2AJF (X-ray 2.9 Å) (20)
		NTD (1–615)	RBD (306–515)	185 nM	SPR			
		NTD (19–615)	RBD (306–527)	408.7 ± 11 nM	SPR			
		NTD (1–614)	S1 (1–676)	15 nM	BLI			
hDPP4 (or CD26)	MERS-CoV S	hDPP4 (39–766)	RBD (367–606)	12 nM	SPR	Residues in the β-propeller domain at the N terminus of DPP4 interact with MERS-CoV RBD domain.	Mutation Tyr499Ala in MERS-CoV S disrupts binding to DPP4.	PDB ID: 4L72 (X-ray 3 Å) (16)
		hDPP4 (39–766)	RBD (36–606)	6.4 ± 0.8 nM	SPR			

Abbreviations: aa, amino acid; BLI, biolayer interferometry; CoV, coronavirus; CoV S, Spike glycoprotein situated on the surface of SARS-CoV, SARS-CoV-2, and MERS virus that interacts with host receptors; cryo-EM, cryo-electron microscopy; CTD, C-terminal domain; DPP4, dipeptidyl peptidase 4; EMBD ID, Electron Microscopy Data Bank Identifier; hACE2, human angiotensin-converting enzyme 2; human/civet, N-terminal helix from civet and the peptidase domain from human; K_d, dissociation constant; MERS, Middle East respiratory syndrome; NA, not available; NTD, N-terminal domain; PDB ID: Protein Data Bank Identifier; RBD, receptor binding domain; S, Spike glycoprotein; SARS, severe acute respiratory syndrome; SARS-CoV-2 S trimer, residues 1–1208 with residues 986 and 987 substituted with prolines, a GSAS substitution at the furin cleavage site residues 682–685, and a fused C-terminal T4 fibritin trimerization motif; SPR, surface plasmon resonance.

characterization and complex structures of small-molecule inhibitors (PDB IDs: 6LZE, 7BQY, 7BUY, 6Y2F, 7BV2) (21–24) that target various pathways of the virus—entry, replication, and assembly—have been determined and can be used to elucidate how these molecules act as therapeutic agents against SARS-CoV-2 (**Table 2**). Taking cues from available virus S-glycoprotein–human receptor interactions, this review seeks to provide a mechanistic basis for receptor usage by SARS-CoV, MERS-CoV, and SARS-CoV-2. Learning from SARS-CoV- and MERS-CoV-associated therapies, we also analyze the molecular basis of blocking SARS-CoV-2 by various therapeutic small-molecule drugs. Thus, this article provides a foundation for the development of new therapeutic and preventive strategies, and proposes potential ways to improve existing strategies, such as vaccines and antibodies, and the use of small-molecule drugs, against COVID-19.

PIKfyve: phosphatidylinositol 3-phosphate 5-kinase

TPC2: two-pore channel subtype 2

hACE2: human ACE2

TMPRSS2: transmembrane serine protease 2

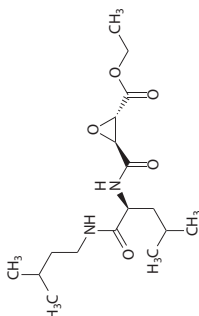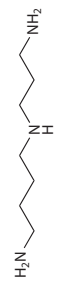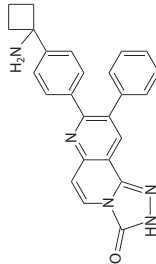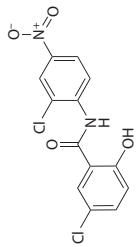## 2. SARS-COV-2, SARS-COV, AND MERS-COV ENTRY MECHANISM
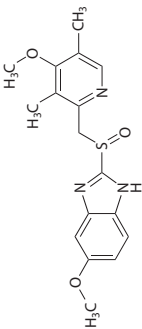
Viruses enter hosts by fusion or endocytosis. During fusion, the virus attaches to and connects with the cell membrane, a process mediated by the binding of viral proteins (S-glycoproteins) to host cell receptors [human ACE2 (hACE2) or DPP4]. This leads to the formation of an immune-resistant protein complex that can cross membrane barriers. In contrast, in receptor-mediated endocytosis, the viral particle attaches to the cell membrane using S-glycoproteins as attachment factors and is engulfed by the cell membrane as vesicles, a process mediated by the host cell receptors (25). In 2020, Qian and colleagues (10) demonstrated that SARS-CoV-2 enters host cells via endocytosis. The authors (10) suggested that phosphatidylinositol 3-phosphate 5-kinase (PIKfyve), two-pore channel subtype 2 (TPC2), and cathepsin L are crucial for SARS-CoV-2 entry. By comparison, SARS-CoV enters host cells via a clathrin- and caveolae-independent, receptor- and pH-dependent mechanism of endocytosis (26). Using confocal microscopy, Jiang and colleagues (26) showed that hACE2 translocates from the cell surface into intracellular compartments after treatment with pseudovirus harboring the S-glycoprotein in SARS-CoV. The transmembrane serine protease 2 (TMPRSS2) is thought to cleave the SARS-CoV S-glycoprotein after it undergoes a conformational change upon binding to hACE2, exposing the cleavage site near the C terminus (27, 28). MERS-CoV entry into the host is dependent on cysteine protease cathepsin L in the presence of uncleaved pseudovirions (29, 30). Using guided protease expression and inhibition assays, Pöhlmann and colleagues (30, 31) and Nagata and colleagues (32) showed that TMPRSS2 activates the S-glycoprotein in human coronavirus EMC (hCoV-EMC) and mediates cathepsin B/L-independent host cell intrusion, similar to the mode of entry described for SARS-CoV.

3. SEQUENCE FEATURES AND HIGHER TRANSMISSIBILITY EXHIBITED BY SARS-COV-2

SARS-CoV-2 harbors an Arg-rich multibasic cleavage site (also known as the RRAR furin cleavage site) that is sensitive to furin, an enzyme present in host cells (3, 12, 33). This site is not found on SARS-CoV. Through mutational analysis, Pöhlmann and colleagues (34) confirmed that the furin cleavage site must remain intact for high-efficiency proteolytic processing of the SARS-CoV-2 S-glycoprotein and efficient entry into host cells. The addition of an Arg residue along with an Ala-to-Lys replacement in the SARS-CoV-2 S-glycoprotein showed no enhanced cleavability (34). Thus, the multibasic furin cleavage site in SARS-CoV-2 S-glycoprotein appears to be necessary for high-fidelity proteolytic processing.
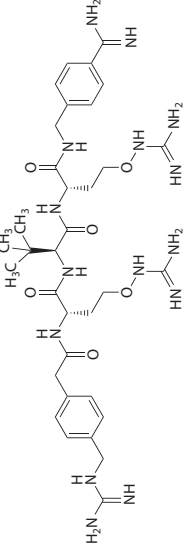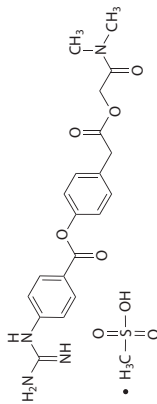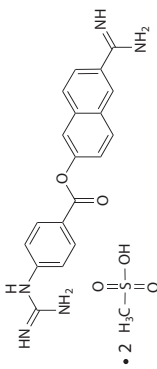
During viral infection, syncytia formation is a phenomenon that occurs when infected cells fuse with neighboring cells to result in large, multinucleated cells. To establish the critical role of

Table 2 Inhibitors targeting viral entry and fusion

Compound [reference(s)] MW (g/mol)[a] Target region	Chemical structure	IC$_{50}$ value and function	Status of therapeutic developments	IC$_{50}$, CC$_{50}$, EC$_{50}$, and SI values
Omeprazole (8) MW: 345.40 Lysosome		SARS-CoV-2: 34 μM SARS-CoV: 26.8 μM As a proton pump inhibitor, increases pH in the lysosome Inhibits double-stranded RNA formation	Repurposed drug SARS-CoV-2: in vitro experiments	CC$_{50}$ > 80 μM
E-64d (10, 75, 76) MW: 342.43 Lysosomal cathepsin and calpain		NA Inhibits lysosomal cathepsin B/L and blocks the cathepsin/endosome entry pathway of SARS-CoV-2	Repurposed drug SARS-CoV-2: in combination with camostat mesylate; in vitro experiments	NA
Spermidine (61) MW: 145.25 Autophagy pathway		SARS-CoV-2: 149 μM Acts as an autophagy inducer, enhances autophagy, and inhibits SARS-CoV-2 propagation	Repurposed drug SARS-CoV-2: in vitro experiments	NA
MK-2206 (61) MW: 407.50 Autophagy pathway		SARS-CoV-2: 90 nM Inhibits AKT1, enhances autophagy, and inhibits SARS-CoV-2 propagation	Repurposed drug SARS-CoV-2: in vitro experiments	NA
Niclosamide (61, 93, 156) MW: 327.12 Autophagy pathway		SARS-CoV-2: 170–280 nM Inhibits E3-ligase SKP2, enhances autophagy, and inhibits SARS-CoV-2 propagation	Repurposed drug SARS-CoV-2: in vitro experiments	NA

(Continued)

Table 2 (Continued)

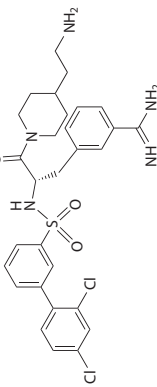| Compound [reference(s)] MW (g/mol)[a] Target region	Chemical structure	IC$_{50}$ value and function	Status of therapeutic developments	IC$_{50}$, CC$_{50}$, EC$_{50}$, and SI values
MI-1851 (96) MW: 767.90 Furin protease		NA Prevents virus entry by inhibiting furin cleavage at S1/S2 site of S-glycoprotein	Repurposed drug SARS-CoV-2: in vitro experiments	NA
Camostat mesylate (8, 33, 102, 157) MW: 494.50 TMPRSS2 protease		SARS-CoV-2: 1.2 μM SARS-CoV: 16.7 μM Partially blocks SARS-CoV-2-S- and SARS-CoV-driven entry by inhibiting the protease TMPRSS2 Fully blocks the SARS-2-S-driven entry when applied with inhibitor E-64d	Repurposed drug SARS-CoV-2: in clinical trial	SARS-CoV-2: EC$_{50}$ = 87 nM SARS-CoV: EC$_{50}$ = 198 nM CC$_{50}$ > 200 μM
Nafamostat mesylate (76, 102, 103) MW: 539.60 TMPRSS2 protease		SARS-CoV-2: 0.49 μM SARS-CoV: 18.9 μM Prevents S-glycoprotein activation by inhibiting TMPRSS2 protease	Repurposed drug SARS-CoV-2: in clinical trial	SARS-CoV-2: EC$_{50}$ = 5 nM SARS-CoV: EC$_{50}$ = 1.4 nM CC$_{50}$ > 200 μM
Aprotinin (8, 96, 158) MW: 6511.51 TMPRSS2 protease	N'-RPDFCLEPPYTGPCKARIIRY FYNAKAGLCQTFVYGGCRA KRNNFKSAEDCMRTCGGA-C'	SARS-CoV-2: 22.9 KIU/ml SARS-CoV: 118 KIU/ml Prevents virus entry by inhibiting TMPRSS2 cleavage at the S2 site of S-glycoprotein Inhibits double-stranded RNA formation in SARS-CoV-2 infected cells	Repurposed drug SARS-CoV-2: in vitro experiments	CC$_{50}$ > 1,000 KIU

(Continued)

Table 2 *(Continued)*

Compound [reference(s)] MW (g/mol)[a] Target region	Chemical structure	IC$_{50}$ value and function	Status of therapeutic developments	IC$_{50}$, CC$_{50}$, EC$_{50}$, and SI values
MI-432 (96, 105) MW: 573.57 TMPRSS2 protease		NA Prevents virus entry by inhibiting TMPRSS2 cleavage at S2 site of S-glycoprotein	Repurposed drug SARS-CoV-2: in vitro experiments	NA
EK1C4 (107) MW: 5258.06 S-glycoprotein	N′-EK1–GSGSG–PEG4–Chol-C′, where EK1 is N′-SLDQINVTFLDLEYEMKKLE EAIKKLEESYIDLKEL-C′	SARS-CoV-2 S-glycoprotein–mediated membrane fusion: 1.3 nM SARS-CoV-2 pseudovirus: 15.8 nM Live SARS-CoV-2: 36.5 nM Inhibits cell–cell fusion by binding to HR1 region in the S2 subunit of S-glycoprotein and prevents formation of the 6-HB fusion core structure	New drug SARS-CoV-2: in vitro and in vivo experiments	CC$_{50}$ > 5 μM SI > 136
IPB02 (109) MW: 4408.23 S-glycoprotein	N′-ISGINASVVNIQKEIDRLNEV AKNLNESLIDLQELK(Chol)-C′	SARS-CoV-2 S-glycoprotein–mediated membrane fusion: 25 nM SARS-CoV-2 pseudovirus: 80 nM SARS-CoV-pseudovirus: 251 nM Inhibits cell–cell fusion by binding to HR1 region in the S2 subunit of S-glycoprotein and prevents formation of the 6-HB fusion core structure	New drug SARS-CoV-2: in vitro experiments	NA

[a]The molecular weights for MI-1851 and MI-432 are calculated on the basis of the chemical structure; the molecular weights for aprotinin, EK1C4, and IPB02 are computed from ExPASy (http://web.expasy.org); and the molecular weights for omeprazole, E-64d, spermidine, MK-2206, niclosamide, camostat mesylate, and nafamostat mesylate are obtained from PubChem (https://pubchem.ncbi.nlm.nih.gov).

Abbreviations: 6-HB, six-helix bundle; Chol, cholesterol; HR1, heptad repeat 1; KIU, Kallikrein inactivator unit; MERS-CoV, Middle East respiratory syndrome-related coronavirus; MW, molecular weight; NA, not available; S-glycoprotein, Spike glycoprotein; SARS-CoV-2, severe acute respiratory syndrome-related coronavirus-2; SI, selective index; SKP2, S-phase kinase-associated protein 2; TMPRSS2, transmembrane serine protease 2.

the multibasic furin cleavage site in syncytia formation, Pöhlmann and colleagues (34) performed mutational experiments and syncytia formation assays. SARS-CoV-2 S-glycoprotein and MERS-CoV S-glycoprotein showed syncytia formation, which increased in the presence of trypsin and the expression of TMPRSS2. In the absence of the multibasic furin cleavage site, syncytia formation was remarkably reduced, even in the presence of trypsin or TMPRSS2. Whereas SARS-CoV wild type expression did not establish syncytia formation, SARS-CoV wild type in the presence of furin cleavage sites showed syncytia formation and enhanced cell–cell fusion (35). Overall, these findings reveal the importance of the furin cleavage site in cell–cell fusion and high-fidelity proteolytic processing and suggest the utility of inhibitors targeting furin or TMPRSS2 as potential therapeutic options.

The dissociation constant (K_d) value of the SARS-CoV-2 RBD/hACE2 interaction is in the lower nanomolar range (18, 19) (**Table 1**). This strong affinity could be another reason why SARS-CoV-2 spreads faster than other coronaviruses.

Moreover, SARS-CoV-2 infects people of different age groups and demographics, but differences in infectivity and severity between men and women and between adults and children are reported (36). This disparity may be attributed to the difference in hACE2 expression among different age groups and gender. hACE2 expression is believed to be higher in men because the *ACE2* gene is located on the X chromosome (36). In a comparison of adults and children, enhanced hACE2 expression was observed in well-differentiated cells (adults) but not in poorly differentiated cells (children) (36, 37). Though suggestive, these claims need substantiation with further experimental evidence.

4. STRUCTURAL INSIGHTS INTO VIRUS–RECEPTOR INTERACTIONS

Biochemical characterization and structural analysis have provided insights into the molecular conformations of hACE2 and human DPP4 (hDPP4) and clues about how they interact with the S-glycoprotein. hACE2 comprises an active N-terminal peptidase domain with two lobes, resembling a claw-like structure, and a C-terminal collectrin domain that can assume both opened and closed conformations (38). The SARS-CoV RBD can bind to hACE2 irrespective of the conformation assumed by hACE2 (20). Four key residues in hACE2 govern the interaction—Lys31, Glu35, Asp38, and Lys353—of which Glu35 is conserved across numerous species (e.g., domestic cats, ferrets, monkeys, and raccoons) (11).

The human host cell receptor hDPP4 consists of an N-terminal eight-bladed β-propeller domain (39–496), with each blade formed by four antiparallel β-strands and a C-terminal hydrolase domain (497–766) (16). The hDPP4 blades interact with MERS-CoV. Akin to the SARS-CoV S-glycoprotein, the MERS-CoV S-glycoprotein comprises an NTD and an RBD consisting of 84 residues folded into four-stranded antiparallel β-sheets [amino acids (aa) 484 to 567] (16). Several key residues in the hDPP4 β-propeller domain (Val26, Arg336, and Arg317) interact with the MERS-CoV RBD residues (Asp510, Glu536, Asp537, and Asp539) through a network of hydrophilic and hydrophobic interactions (16).

SARS-CoV-2 and MERS-CoV have a furin cleavage site and are cleaved for attachment and pathogenesis. During fusion with the host, the S1 and S2 subunits of the MERS-CoV S-glycoprotein separate. The S2 subunit forms a six-helix bundle [(6-HB), with a heptad repeat 1 (HR1) (aa 987–1062) and HR2 (aa 1263–1279) region] that fuses with the host cell membrane (39). SARS-CoV and MERS-CoV have high sequence identity in the NTD but poor conservation of the RBD, which may explain their different host cell receptor specificity (16).

As does the S-glycoprotein of SARS-CoV, the S-glycoprotein of SARS-CoV-2 engages with hACE2 under neutral pH conditions for fusion and entry into host cells (18–20, 40). The SARS-CoV-2 S-glycoprotein has 22 *N*-linked glycosylation sites that are spread throughout the different

domains, including the NTD (at positions 1, 4, 122, 149, 165, 234, and 282) and RBD (at positions 331 and 343) (41). An analysis of the X-ray and cryo-EM structures published by different groups points to the RBD as the key region that interacts with hACE2 (**Table 1**) in a 1:1 ratio (one SARS-CoV-2 RBD molecule binding to one hACE2 receptor molecule); the SARS-CoV-2 NTD, in the absence of RBD, is unable to bind to hACE2 (2).

The SARS-CoV-2 RBD consists of five antiparallel β-sheets (β1, β2, β3, β4, and β7), and two short β-strands (β5 and β6) situated between β4 and β7, connected by short helices (α4 and α5) and loops (18). Most of the hACE2-interacting residues lie in the region formed by α4-and α5-helices, β5- and β6-sheets, and the connecting loops, collectively labeled as the receptor binding motif (RBM) (2, 18, 19). More than 16 residues in the RBD interact with hACE2: 8 residues are unique to SARS-CoV and 9 to SARS-CoV-2 (18) (**Figure 1c**). Conversely, 21 key residues in hACE2 interact with the RBD, with only 1 and 2 residues unique to SARS-CoV-2 and SARS-CoV, respectively (2) (**Figure 1d**). Superimposition of the RBD structures of SARS-CoV and SARS-Cov-2 shows a root-mean-square deviation value of 0.475 Å for 128 equivalent Cα atoms (2).

In addition to the hydrogen bonding contacts, there is a network of hydrophobic interactions formed by residues Phe486 and Tyr489 in SARS-CoV-2 RBD and by residues Phe28, Leu79, Met82, and Tyr83 in hACE2 (2). A key receptor-interacting residue, Lys417, situated outside the SARS-CoV-2 RBM, forms a salt bridge with Asp30 of hACE2. For SARS-CoV RBD, Lys417 is replaced by a valine residue, which does not interact with hACE2 (18).

In the SARS-CoV-2 RBM, an hACE2-interacting loop (a four-residue motif, GVEG) adopts a favorable conformation for binding, which differs from that in the SARS-CoV RBM (a three-residue motif, PPA) (2, 19). Mutations introduced into the hACE2 binding loop of the SARS-CoV-2 RBM reduce its affinity, confirming the critical role of the loop in receptor binding (19).
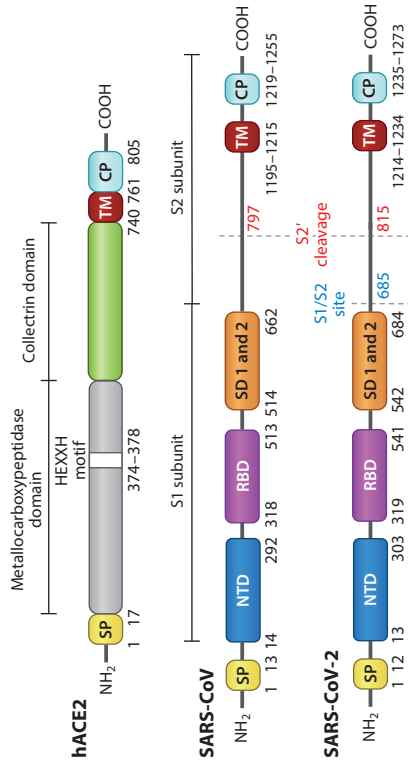
The nanomolar range of the binding affinity between hACE2 and the SARS-CoV-2 RBD—as determined by surface plasmon resonance and biolayer interferometry experiments—point to the critical role of the RBD in host cell receptor binding (2). Even though different groups have reported discrepancies regarding the affinity of this binding, presumably due to differences in experimental protocols, all the K_d values are in the nanomolar range. Wang and colleagues (2) reported that the SARS-CoV-2 RBD has a fourfold stronger affinity for hACE2 than does the SARS-CoV RBD. This could be due to the different conformational states adopted by the SARS-CoV S-glycoprotein: its receptor-binding inactive state and active state. In the inactive state, the RBDs point downward, which causes a steric clash that inhibits its interaction with hACE2. In contrast, in the active conformation, the RBDs point upward, presenting the binding site and thus facilitating hACE2 binding (46, 47).

Although the mode of binding exhibited by the RBD to hACE2 is comparable between the two viruses (18), the RBM of the SARS-CoV-2 S-glycoprotein forms a broader binding interface, establishing more contacts with hACE2 (2, 19). This might explain the higher binding affinity of the SARS-CoV-2 RBD to hACE2.

The presence of many hydrophilic interactions, governed by salt bridges and hydrogen bonds, is a common feature between the SARS-CoV-2 RBD/hACE2 and SARS-CoV RBD/hACE2 interfaces (2, 18).

Experiments have been performed to determine whether the antibodies raised against the SARS-CoV S1 subunit could neutralize SARS-CoV-2. Most results have been disappointing, with little to no cross-neutralization for many of the antibodies, indicating that there are likely to be crucial differences in antigenicity (2). But some SARS-CoV-2- and SARS-CoV-derived antibodies (48–50) have shown promising neutralizing activities against SARS-CoV-2. Because the SARS-CoV and SARS-CoV-2 S-glycoproteins bind to ACE2 and not hDPP4, which is specific

a hACE2, SARS-CoV, SARS-CoV-2

hACE2

NH$_2$ — SP — NTD — RBD — SD 1 and 2 — TM — CP — COOH

Metallocarboxypeptidase domain
HEXXH motif
Collectrin domain
S1 subunit
S2 subunit

1 17   374–378   740 761 805
292 318   513 514   662
1195–1215 1219–1255

SARS-CoV

NH$_2$ — SP — NTD — RBD — SD 1 and 2 — TM — CP — COOH

S2' cleavage 797
S1/S2 site 685

SARS-CoV-2

NH$_2$ — SP — NTD — RBD — SD 1 and 2 — TM — CP — COOH

1 12 13   303 319   541 542   684   815   1214–1234 1235–1273

b hDPP4, MERS-CoV

hDPP4

NH$_2$ — CP — TM — COOH

β-propeller domain
α/β hydrolase domain
DPP4 catalytic site

1 6 29   340–343 (ADA)   469–479 (Fibronectin)   496   S630 D708 H740 766
S1/S2 cleavage 751

MERS-CoV

NH$_2$ — SP — NTD — RBD — SD 1 and 2 — TM — CP — COOH

S1 subunit   S2 subunit
1 17 18   350 381   588 595   751   887   1296–1318 1319–1353
S1/S2 cleavage   S2' cleavage

c Structure-based sequence alignment of RBD

SARS-CoV RBD 319 ITNLCPFGEVFNATKFPSVYAWERKKISNCVADYSVLYN STFSTFKCYG 368
SARS-CoV-2 RBD 332 ITNLCPFGEVFNATRFASVYAWNRKRISNCVADYSVLYNSASFSTFKCYG 381

SARS-CoV RBD 369 VSATKLNDLCFSNVYADSFVVKGDDVRQIAPGQTGVIADYNYKLPDDFMG 418
SARS-CoV-2 RBD 382 VSPTKLNDLCFTNVYADSFVIRGDEVRQIAPGQTGKIADYNYKLPDDFTG 431

Key residue

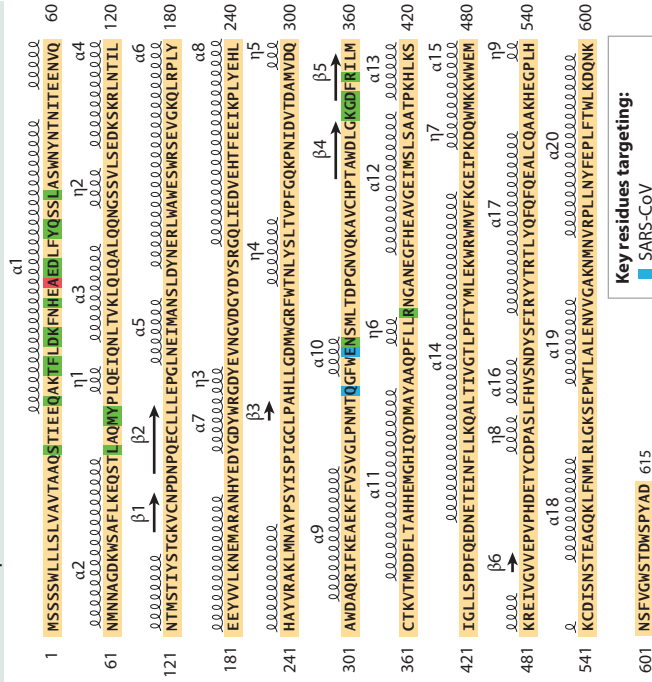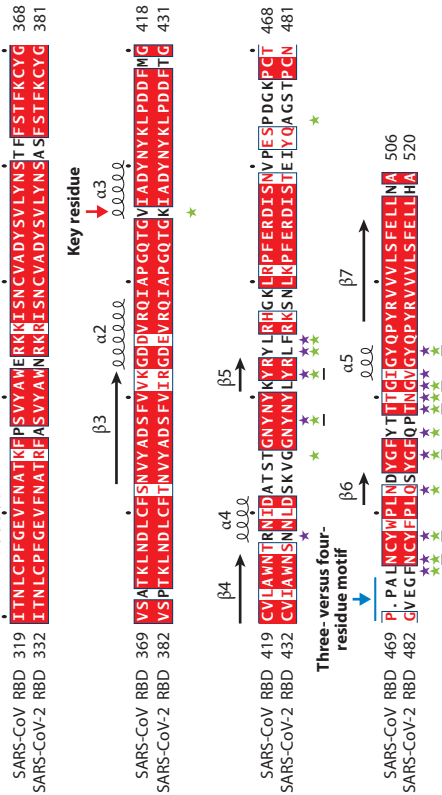SARS-CoV RBD 419 CVLAWNTRNIDATSTGNYNYKYRYLRHGKLRPFERDISNVPFSPDGKPCT 468
SARS-CoV-2 RBD 432 CVIAWNSNNLDSKVGGNYNYLYRLFRKSNLKPFERDISTEIYQAGSTPCN 481

Three- versus four-residue motif

SARS-CoV RBD 469 PI.PALNCYWPLNDYGFYTTGIGYQPYRVVVLSFELLNA 506
SARS-CoV-2 RBD 482 GVEGFNCYFPLQSYGFQPTNGVGYQPYRVVVLSFELLHA 520

α1 α2 β1 β2 β3 α3 β4 α4 β5 β6 β7 α5

Key residue

ACE2-binding residues of:
★ SARS-CoV
★ SARS-CoV-2
— Conserved residues

Helix β-strand

d hACE2–Spike interaction

1 MSSSSWLLLSLVAVTAAQSTIEEQAKTFLDKFNHEAEDLFYQSSLASWNYNTNITEENVQ 60
α1 α2

61 NMNNAGDKWSAFLKEQSTLAQMYPLQEIQNLTVKLQLQALQQNGSSVLSEDKSKRLNTII 120
η1 α3 η2 α4

121 NTMSTIYSTGKVCNPDNPQECLLLEPGLNEIMANSLDYNERLWAWESWRSEVGKQLRPLY 180
β1 β2 α5 α6

181 EEYVVLKNEMARANHYEDYGDYWRGDYEVNNGVDGYDYSRGQLIEDVEHTFEEIKPLYEHL 240
η3 β3 α7 η4 α8

241 HAYVRAKLMNAYPSYISPIGCLPAHLLGDMWGREFWTNLYSLTVPFGQKPNIDVTDAMVDQ 300
α9 α10 η5

301 AWDAQRIFKEAEKFFVSVGLPNMTQGFWENSMLTDPGNVQKAVCHPTAWDLGKGDFRILM 360
α11 η6 α12 α13 β4 β5

361 CTKVTMDDFLTAHHEMGHIQYDMAYAAQPFLLRNGANEGFHEAVGEIMSLSAATPKHLKS 420
α14 η7 α15

421 IGLLSPDFQEDNETEINFLLKQALTIVGTLPFTYMLEKWRWMVFKGEIPKDQWMKKWWEM 480
α16 α17 η8 η9

481 KREIVGVVEPVPHDETYCDPASLFHVSNDYSFIRYYTRTLYQFQFQEALCQAAKHEGPLH 540
α18 α19 α20

541 KCDISNSTEAGQKLFNMLRLGKSEPWTLALENVVGAKNMNVRPLLNYFEPLFTWLKDQNK 600

601 NSFVGWSTDWSPYAD 615

Key residues targeting:
SARS-CoV
SARS-CoV-2
SARS-CoV and SARS-CoV-2

(Caption appears on following page)

Figure 1 (*Figure appears on preceding page*)

Domain architecture and comparison of host cell receptors (hACE2 and hDPP4), SARS-CoV, and SARS-CoV-2. (*a*) Domain organization of the SARS-CoV and SARS-CoV-2 S-glycoprotein and host cell receptor hACE2. (*b*) Domain organization of the MERS-CoV S-glycoprotein and host cell receptor hDPP4. (*c*) Structure-based sequence alignment of SARS-CoV RBD and SARS-CoV-2 RBD. (The RBD is also known as the CTD.) The secondary structures (α for helix, η for 310 helix, and β for strand) are assigned on the basis of PDB ID: 6M0J (SARS-CoV-2 S RBD). Strictly conserved residues are highlighted in red and similar residues are in red letters. SARS-CoV and SARS-CoV-2 residues interacting with hACE2 are indicated with a purple star and a green star, respectively. The conserved residues in SARS-CoV-2 and SARS-CoV that bind to hACE2 are underlined in black. The key residue Lys417 in SARS-CoV-2 and its equivalent, valine in SARS-CoV, are indicated with a red arrow. The three-residue motif in SARS-CoV and four-residue motif in SARS-CoV-2 are indicated with a blue arrow. The structure-based sequence alignment was obtained by DALI (42); subsequently, ClustalW (43) and ESPript (44) were used. Each black dot above the sequence represents 10 amino acids. (*d*) hACE2 (1–615 aa) secondary structures were assigned by STRIDE (45) with PDB ID: 1R42, and the secondary structures helix (*spirals*) and β-strands (*arrows*) are indicated above the sequence. The key residues targeting SARS-CoV and SARS-CoV-2 are highlighted in blue and red, respectively. Conserved residues in hACE2 that bind to SARS-CoV and SARS-CoV-2 are highlighted in green. Abbreviations: aa, amino acid; ADA, adenosine deaminase; CP, cytoplasmic tail; CTD, C-terminal domain; FP, fusion peptide; NTD, N-terminal domain; hACE2, human angiotensin-converting enzyme 2; hDPP4, human dipeptidyl peptidase 4; MERS-CoV, Middle East respiratory syndrome-related coronavirus; PDB ID, Protein Data Bank Identifier; RBD, receptor binding domain; S, Spike; SARS-CoV, severe acute respiratory syndrome-related coronavirus; SD, subdomain; SP, signal peptide; TM, transmembrane.

for MERS-CoV (2), it is unlikely that any of the MERS-CoV antibodies will offer any protection against SARS-CoV and SARS-CoV-2.

Analyses of the published mutational studies, flow cytometry, colocalization, biochemical data, and structures have suggested that the SARS-CoV-2 S-glycoprotein shows a more favorable interaction with hACE2 than does the SARS-CoV S-glycoprotein. Although the structures of the S-glycoprotein–receptor complexes are similar, it remains unclear whether structural differences are the sole reason for the faster transmissibility of SARS-CoV-2 between hosts. Another important finding to consider is the difference in the antigenicity and immunogenicity between SARS-CoV-2 and SARS-CoV S-glycoproteins.

5. CURRENT STATUS OF POTENTIAL SMALL-MOLECULE COMPOUNDS AVAILABLE AGAINST SARS-COV-2
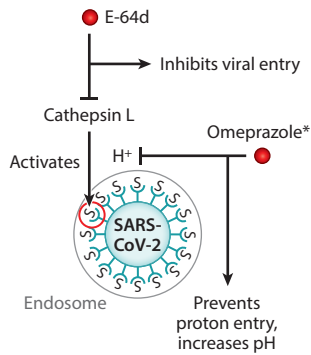
There is no effective drug or vaccine currently available for COVID-19. Clinically approved drugs with published safety profiles represent the fastest option to discover an effective therapy, particularly during a pandemic. Clinically approved drugs are being repurposed as potential treatment options for COVID-19 (51, 52).

Several reports suggest new compounds and repurposed drugs appear to have great potential against SARS-CoV-2 infection. Some of these candidates were also tested against SARS-CoV and MERS-CoV. These antivirals exert their activity by inhibiting viral entry and fusion pathways, blocking viral proteases important for viral transcription, and targeting host factors that are essential for viral replication (**Figures 2** and **3**). In this section and in **Tables 2** and **3**, we discuss the current status of potential drugs available for this ongoing pandemic of SARS-CoV-2.
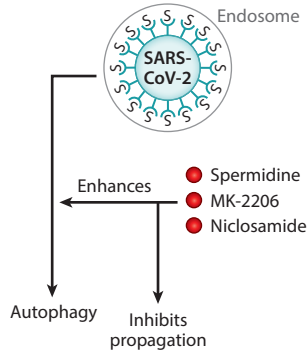
5.1. Targeting Viral Entry via the Endosomal Pathway

Following hACE receptor binding and endocytosis, acidification of the internalized endosome is required to retrieve the internalized cargo proteins and viral RNAs that support coronavirus replication (53–56). Lysosomal cathepsins are essential for SARS-CoV-2, SARS-CoV, and MERS-CoV entry via endocytosis (10). Fusion activation by cathepsin L cleavage of the SARS-CoV-2 S-glycoprotein is similar to that observed for SARS-CoV and MERS-CoV (10, 29, 57).
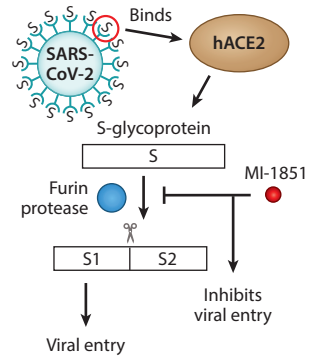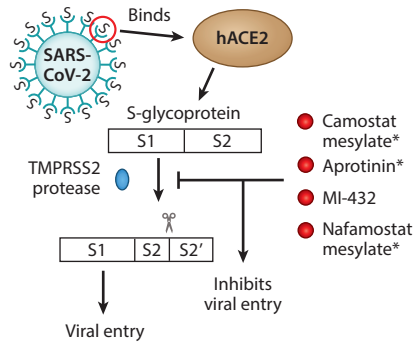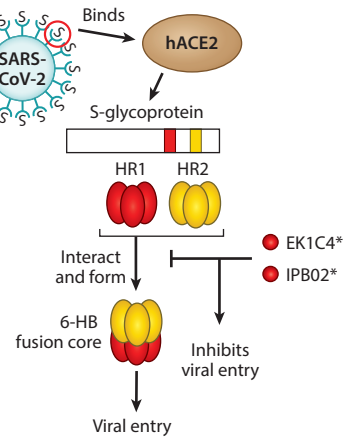
a

i Cathepsin L

E-64d

→ Inhibits viral entry

Cathepsin L

Activates | H⁺ ⊣ Omeprazole*

Endosome

Prevents proton entry, increases pH

ii Autophagy

Endosome

SARS-CoV-2

Enhances ← Spermidine, MK-2206, Niclosamide

Autophagy | Inhibits propagation

iii Furin protease

Binds → hACE2

S-glycoprotein

S

Furin protease | MI-1851

S1 | S2

Viral entry | Inhibits viral entry

iv TMPRSS2

Binds → hACE2

S-glycoprotein

S1 | S2

TMPRSS2 protease

Camostat mesylate*
Aprotinin*
MI-432
Nafamostat mesylate*

S1 | S2 | S2′

Viral entry | Inhibits viral entry

v HR region

Binds → hACE2

S-glycoprotein

HR1 | HR2

Interact and form | EK1C4*, IPB02*

6-HB fusion core | Inhibits viral entry

Viral entry

b

i Main protease (3CL protease)

Released viral RNA

Translation

Polyprotein (pp1a, pp1ab)

3CL protease

11a and 11b
N3
Carmofur
Ebselen
α-Ketoamide 13b

NSPs

Form | No formation of RdRp and other NSPs

RdRp

Viral replication

ii RdRp

EIDD-1931*, †
EIDD-2801*, †

Mutated

Released viral RNA | RdRp | Replicated viral RNA

Inhibits dsRNA formation

Remdesivir*
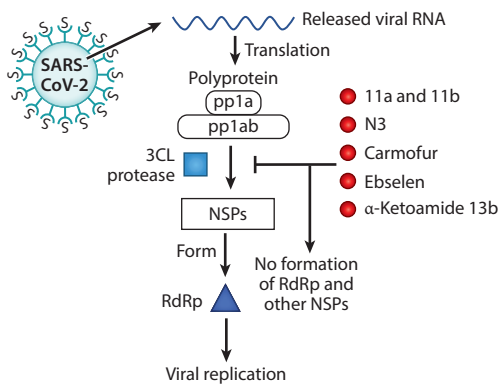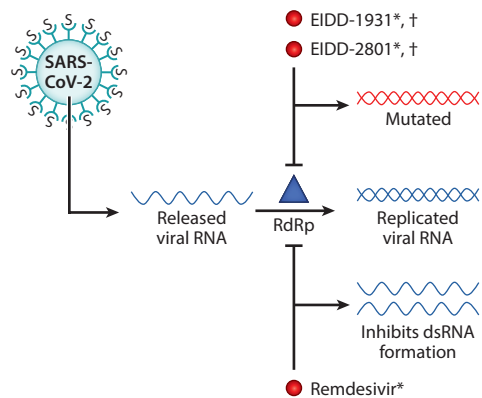
(*Caption appears on following page*)

Figure 2 (*Figure appears on preceding page*)

Blocking of host–pathogen interaction by small-molecule inhibitors. (*a*) Inhibitors (*red spheres*) targeting (*i*) cathepsin L, (*ii*) the autophagy pathway, (*iii*) furin protease, (*iv*) TMPRSS2 protease, and (*v*) formation of the 6-HB fusion core during virus entry and fusion. (*b*) Inhibitors targeting (*i*) main proteases and (*ii*) RdRp during virus replication. Inhibitors targeting SARS-CoV-2 and SARS-CoV are indicated with an asterisk; those targeting SARS-CoV-2 and MERS-CoV are indicated with a dagger. Abbreviations: 3CL, 3C-like; 6-HB, six-helix bundle; dsRNA, double-stranded RNA; hACE2, angiotensin-converting enzyme 2; HR1/2, heptad region 1/2; NSP, nonstructural protein; RdRp, RNA-dependent RNA polymerase; S1, S2, subunit 1, subunit 2; SARS-CoV-2, severe acute respiratory syndrome-related coronavirus 2; TMPRSS2, transmembrane serine protease 2.

The literature has discrepancies regarding the role of autophagy in coronavirus infection (58). Studies have shown that SARS-CoV and MERS-CoV block the fusion of autophagosomes and lysosomes and suppress the autophagy process (59, 60). Induction of autophagy has an antiviral effect on SARS-CoV-2 and MERS-CoV replication (60–62), but exactly how autophagy suppresses viral replication remains to be determined (63).
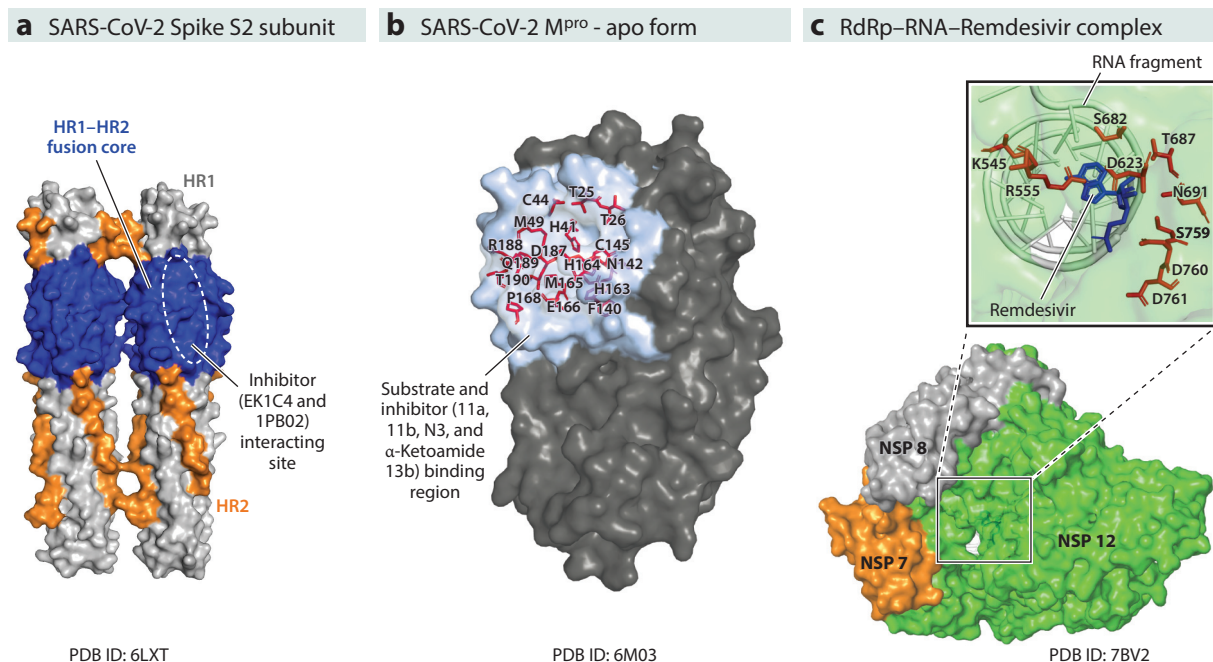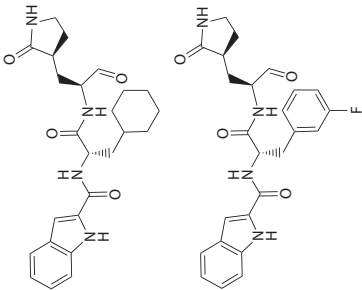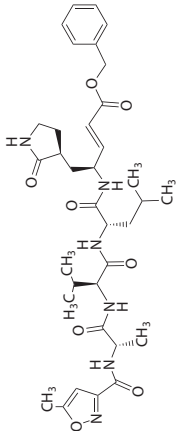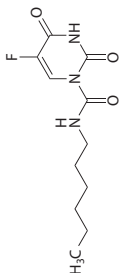

a SARS-CoV-2 Spike S2 subunit
PDB ID: 6LXT

b SARS-CoV-2 M^pro - apo form
PDB ID: 6M03

c RdRp–RNA–Remdesivir complex
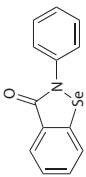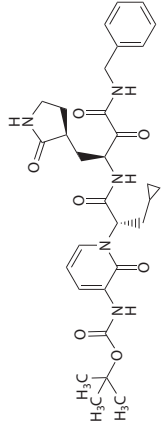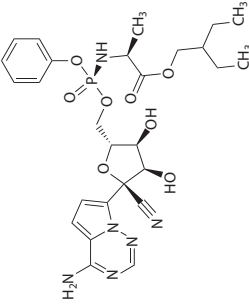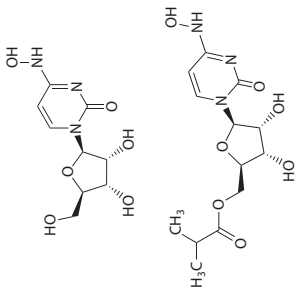PDB ID: 7BV2

Figure 3

Interaction of inhibitors. (*a*) Molecular surface representation of HR in Spike S2 subunit showing HR1 (*gray*) and HR2 (*orange*). The HR1–HR2 fusion core is blue. Inhibitors EK1C4 and IPB02, binding to the HR1–HR2 fusion core, are highlighted with a white-dashed oval. Inhibitors interacting with the HR1–HR2 fusion core prevent formation of the 6-HB core. (*b*) Molecular surface representation of SARS-CoV-2 protease (3CL protease), with the substrate and inhibitor binding region depicted with red sticks. Inhibitors 11a, 11b, N3, and α-ketoamide 13b target the substrate binding region, which in turn inhibits the formation of NSPs, marked in light blue. (*c*) Molecular surface representation of the RdRp–RNA–remdesivir complex. NSP 12, NSP 8, and NSP 7 are highlighted in green, gray, and orange, respectively. NSP 12, NSP 8, and NSP 7 interact to form RdRp. (*Inset*) The RNA fragment and remdesivir are depicted as an image and blue sticks, respectively. The key binding residues of RdRp interacting with remdesivir are depicted as red sticks, and residues are labeled in black. Abbreviation: 6-HB, six-helix fusion bundle; HR1/2, heptad region 1/2; M^pro, main protease; NSP, nonstructural protein; RdRp, RNA-dependent RNA polymerase; SARS-CoV-2, severe acute respiratory syndrome-related coronavirus 2.

Table 3 Inhibitors targeting M^pro and RdRp

Compound [reference(s)] MW (g/mol)[a] Target region	Chemical structure	IC$_{50}$ value and function	Status of therapeutic developments	Structure (resolution) and EC$_{50}$, CC$_{50}$, and SI values
Lead compounds 11a, 11b (21) MW of 11a: 452.56, 11b: 464.50 M^pro		SARS-CoV-2: 40–53 nM Occupies the substrate-binding pocket, covalently binds to Cys145, and blocks the enzyme activity of M^pro	New drug SARS-CoV-2: in vitro and in vivo experiments	PDB ID: 6LZE (1.5 Å) PDB ID: 6M0K (1.5 Å) EC$_{50}$ = 0.53–0.72 μM CC$_{50}$ > 100 μM
N3 (22, 115, 116) MW: 680.35 M^pro		NA Binds to the substrate-binding pocket and irreversibly inhibits M^pro activity	Repurposed drug SARS-CoV-2: in vitro experiments	PDB ID: 6LU7 (2.16 Å) PDB ID: 7BQY (1.7 Å) EC$_{50}$ = 16.77 μM
Carmofur (22, 159) MW: 257.26 M^pro		SARS-CoV-2: 1.82 μM Covalently binds to Cys145 of the catalytic dyad M^pro, completely modifies M^pro	Repurposed drug SARS-CoV-2: in vitro experiments	PDB ID: 7BUY (1.60 Å) EC$_{50}$ = 24.30 μM CC$_{50}$ = 133.4 μM SI = 5.36
Ebselen (22) MW: 274.20 M^pro		SARS-CoV-2: 670 nM Covalently or noncovalently binds to Cys145 of the catalytic dyad M^pro, partially modifies M^pro	Repurposed drug SARS-CoV-2: in vitro experiments	EC$_{50}$ = 4.67 μM

(Continued)

Table 3 *(Continued)*

Compound [reference(s)] MW (g/mol)[a] Target region	Chemical structure	IC$_{50}$ value and function	Status of therapeutic developments	Structure (resolution) and EC$_{50}$, CC$_{50}$, and SI values
α-Ketoamide 13b (23) MW: 580.66 M^{pro}		SARS-CoV-2: 670 nM Binds to substrate-binding pocket	New drug SARS-CoV-2: in vitro and in vivo experiments	PDB ID: 6Y2F (1.95 Å) PDB ID: 6Y2G (2.20 Å) EC$_{50}$ = 4–5 μM
Remdesivir (GS-5734) (8, 24, 154, 160, 161) MW: 602.60 RdRp		SARS-CoV-2: 0.31 μM SARS-CoV: 0.11 μM As an adenosine analog, remdesivir binds to RdRp and incorporates into nascent viral RNA chains and results in premature termination. Inhibits formation of double-stranded RNA	Repurposed drug SARS-CoV-2: in clinical trial Inhibits replication of SARS-CoV and MERS-CoV in tissue culture and nonhuman animal models	PDB ID: 7BV2 (2.5 Å)
NHC (EIDD-1931) (135,143) MW: 259.22 EIDD-2801 (prodrug of NHC) (135, 142) MW: 329.31 RdRp		SARS-CoV-2: 80–300 nM MERS-CoV: 150 nM As a ribonucleoside analog, NHC potently inhibits MERS-CoV and SARS-CoV-2 replication by increasing the mutation rate in viral genomic RNA.	Repurposed drug SARS-CoV-2: in vitro and in vivo experiments Broad-spectrum antiviral activity against SARS-CoV-2, MERS-CoV, SARS-CoV, and related zoonotic group 2b or 2c Bat-CoVs	CC$_{50}$ > 10 μM EIDD-2801: improved oral bioavailability in nonhuman primates

[a]The molecular weights for 11a, 11b, and α-ketoamide 13b are calculated on the basis of the chemical structure; and the molecular weights for N3, carmofur, ebselen, remdesivir, NHC, and EIDD-2801 are obtained from PubChem (**https://pubchem.ncbi.nlm.nih.gov**).

Abbreviations: MERS-CoV, Middle East respiratory syndrome–related coronavirus; M^{pro}, main protease; MW, molecular weight; NA, not available; NHC, β-ᴅ-N^4-hydroxycytidine; PDB ID, Protein Data Bank Identifier; RdRp, RNA-dependent RNA polymerase; SARS-CoV-2, severe acute respiratory syndrome–related coronavirus-2; SI, selective index.

5.1.1. Drugs targeting endosome acidification.

Lysosomotropic agents, such as hydroxychloroquine, chloroquine, and ammonium chloride, inhibit SARS-CoV-2 and SARS-CoV replication by increasing lysosome pH and thus interfering with virus–cell fusion (64–67). During the early stages of the COVID-19 outbreak, the malaria drugs chloroquine and hydroxychloroquine were among the first few inhibitors to be taken to clinical trials (68–70). However, emerging information has led researchers to question the benefit of these drugs.

Omeprazole is another lysosomotropic agent that has been tested for its efficacy against SARS-CoV-2. Omeprazole is a proton pump inhibitor that interferes with lysosomal activity through inhibition of H^+, K^+-ATPase and resultant alkalization of the phagolysosome, which in turn inhibits virion fusion and thus viral replication (71–73) (**Figure 2a**, **subpanel i**). In addition, omeprazole also inhibits double-stranded RNA formation, thereby preventing viral replication (8). Omeprazole inhibits SARS-CoV-2- and SARS-CoV-induced cytopathogenic effect formation (CPE) at an IC_{50} of 27–34 μM (8). However, those concentrations are beyond the acceptable therapeutic concentration for plasma (74). Combining omeprazole with other inhibitors may produce the desired therapeutic response. A combination of aprotinin and omeprazole at the therapeutic concentration enhances aprotinin-mediated SARS-CoV-2-induced CPE formation by 2.7-fold ($IC_{50} = 10.4$ μM). Simultaneous administration of omeprazole and remdesivir, at therapeutic concentrations, increases remdesivir-mediated inhibition activity by 10-fold ($IC_{50} = 0.023$ μM) (8).

5.1.2. Drugs targeting cathepsin.

E64d, a broad-spectrum cysteine protease inhibitor, targets lysosomal cathepsin. E64d has been widely used in studies of endosome-mediated viral entry (**Figure 2a**, **subpanel i**). For example, E64d reportedly reduces the entry of SARS-CoV-2 pseudovirus into HeLa/hACE2, Calu-3, and MRC-5 cells (75), SARS-CoV-2 S pseudovirus into 293/hACE2 cells by 92% (10), and pseudotyped SARS-CoV S-glycoprotein into 293/hACE2 cells (76). Hoffmann et al. (33) reported that the TMPRSS2 inhibitor camostat mesylate partially blocks SARS-CoV-2 S-glycoprotein-mediated entry into target cells and that combined treatment with E64d could fully block viral entry. As SARS-CoV-2 can utilize both cathepsin L and TMPRSS2 for S-glycoprotein priming (10, 33, 77), E64d has the potential to be developed as an anti-SARS-CoV-2 drug and used in combination with a TMPRSS2 inhibitor to achieve a cumulative antiviral effect. Moreover, many engineered noncovalent peptide inhibitors have shown enhanced specificity and affinity toward cathepsin L (78–81).

5.1.3. Drugs targeting the autophagy pathway.

Spermidine is a natural polyamine that induces autophagy (82–85) (**Figure 2a**, **subpanel ii**). Its concentration declines in response to SARS-CoV-2-induced inhibition of spermidine synthase (61). Gassen et al. (61) reported that the supplementation of spermidine can enhance autophagy and suppress SARS-CoV-2 propagation in vitro by 85%. Polyamines also play pivotal roles in viral genome synthesis, including transcription, translation, and genome packaging (63). Studies of chikungunya, Zika, hepatitis C, and Ebola viruses highlight the enhancement of viral polymerase activity by polyamines (86–89). Further investigation is needed to understand the role(s) of spermidine in SARS-CoV-2 infection.

AKT1, which can be inhibited by MK-2206, targets Beclin-1, an autophagy-inducing protein (90, 91). Inhibition of AKT1 by MK-2206 upregulates Beclin-1 and promotes autophagy. Thus, MK-2206 may be a promising drug candidate for the treatment of SARS-CoV-2 infection. MK-2206 reduced SARS-CoV-2 propagation by 88% (61).

Gassen et al. (60) reported that MERS-CoV replication could be reduced by inhibiting S-phase kinase-associated protein 2 (SKP2), an E3-ligase that suppresses autophagy via Beclin-1-mediated ubiquitination. Recently, a paper published by the same group identified niclosamide—an orally bioavailable, chlorinated salicylanilide used to treat tapeworm infestations—as a potential

anti-SARS-CoV-2 agent (61). Niclosamide inhibits SKP2, stabilizes Beclin-1, and enhances autophagy (60, 61). Niclosamide is also a protonophore that blocks endosomal acidification, which is essential for virion fusion (92). Another group also reported antiviral activity of niclosamide against SARS-CoV-2 (IC_{50} = 280 nM) (93). As a US Food and Drug Administration (FDA)-approved anthelmintic drug used in humans for more than 40 years (94, 95), niclosamide has a known safety profile and can be tested in animal models and clinical trials for its efficacy against SARS-CoV-2.

5.2. Targeting Viral Entry Through the Plasma Membrane Fusion Pathway

The plasma membrane fusion pathway is an essential part of viral infection and thus a candidate target for virus pathogenicity. Unlike most betacoronaviruses, the S-glycoprotein of SARS-CoV-2 has a multibasic S1/S2 proprotein convertase furin cleavage site (34). In the plasma membrane fusion pathway, SARS-CoV-2 uses furin and the TMPRSS2 serine protease for S-glycoprotein priming: Furin cleaves S-glycoprotein at the S1/S2 site, whereas TMPRSS2 targets the S2 site (34, 96). Hence, TMPRSS2 is a target for serine protease inhibitors to block S-glycoprotein cleavage and viral entry. Both furin and TMPRSS2 are essential and cannot compensate for each other in S-glycoprotein activation (96). Therefore, drugs targeting either (or perhaps both) of these proteases involved in the plasma membrane fusion pathway may suppress S-glycoprotein activation and viral entry.

During viral pathogenesis, membrane fusion is instigated by the formation of the 6-HB fusion core. Upon hACE2 receptor binding, the HR1 and HR2 domains in the S2 subunit of the S-glycoprotein interact with each other to form the core (97–99); the viral and cell membranes are driven into close proximity by its formation. Thus, inhibitors that target formation of the 6-HB fusion core may also prove useful against membrane fusion to prevent viral entry (**Figures 2a**, **subpanel v** and **3a**).

5.2.1. Drugs targeting furin and TMPRSS2 proteases. Bestle et al. (96) showed that the synthetic furin inhibitor MI-1851 potently inhibits S-glycoprotein cleavage and SARS-CoV-2 replication (**Figure 2a**, **subpanel iii**). In human Calu-3 airway cells infected with SARS-CoV-2, MI-1851 reduced viral titers by 30- to 75-fold, and this effect could be enhanced when delivered in combination with various TMPRSS2 inhibitors (96).

Numerous repurposed TMPRSS2 inhibitors block SARS-CoV-2 S-glycoprotein-mediated entry (**Figure 2a**, **subpanel iv**). Two such inhibitors are camostat mesylate (33), which is approved in Japan for the treatment of pancreatitis (100) and postoperative reflux esophagitis, and nafamostat mesylate, which is approved by the FDA for treating pancreatitis (101). Compared with camostat mesylate, nafamostat mesylate has a >15-fold-lower concentration response (**Table 2**) for inhibition of SARS-CoV-2 entry (102). Nafamostat mesylate has also been identified as a potent inhibitor of MERS-CoV infection (103). Currently, both of these compounds are being evaluated in clinical investigations for the treatment of SARS-CoV-2.

Aprotinin in aerosol form, which delivers drugs directly to the lungs, is approved in Russia for treating influenza (104). Bojkova et al. (8) reported that, at therapeutic concentrations, aprotinin shows higher inhibition of SARS-CoV-2 than of SARS-CoV infection. This might be due to the differentially conserved amino acid positions between the S-glycoproteins of SARS-CoV-2 and SARS-CoV (8). In addition, aprotinin shows a higher antiviral effect than either camostat mesylate or nafamostat mesylate, and in contrast to those compounds, aprotinin also interferes with formation of double-stranded RNA, thereby preventing viral infection in SARS-CoV-2-infected

cells (8). Aprotinin may thus be a promising drug candidate, based on its efficacy at therapeutic concentration and its safety in terms of its mode of administration.

Another serine protease inhibitor, MI-432, is a synthetic peptide mimetic inhibitor of TMPRSS2 (105). MI-432 suppresses SARS-CoV-2 multiplication and CPE in human Calu-3 airway cells. In addition, the combination of MI-432 and the furin inhibitor, MI-1851, has an increased anti-SARS-CoV-2 activity compared with treatment with either inhibitor alone (8).

5.2.2. Drugs targeting HR1 of S2 subunit of S-glycoprotein.

On the basis of the X-ray crystal structure of the 6-HB fusion core of the SARS-CoV-2 S-glycoprotein (PDB ID: 6LXT) and a pan-coronavirus fusion inhibitor EK1 peptide (106), Xia et al. (107) developed a potent fusion inhibitor, EK1C4 lipopeptide, that targets SARS-CoV-2 S-glycoprotein-mediated cell membrane fusion as well as pseudotyped SARS-CoV-2 and live SARS-CoV-2 infection, with IC_{50} values of 1.3, 15.8, and 36.5 nM, respectively. Both EK1 and EK1C4 disrupt formation of the 6-HB fusion core by binding to the HR1 domain and show broad-spectrum fusion-inhibiting activity against SARS-CoV-2, SARS-CoV, and MERS-CoV, as well as against hCoV-OC43, hCoV-NL63, and hCoV-229E (107, 108) (**Figures 2a**, **subpanel v** and **3a**). Upon modification of EK1 with a cholesterol moiety, EK1C4 forms a more stable complex with HR1, which enhances its antiviral activity (149-fold). Furthermore, the high selectivity index of EK1C4 (SI > 136) suggests that it is a potential inhibitor with little to no toxic effect in vitro. IPB02, another lipopeptide fusion inhibitor that targets the HR1 region, was designed on the basis of the HR2 sequence (109). IPB02 also potently inhibits the cell fusion activity of SARS-CoV-2 S-glycoprotein (IC_{50} = 25 nM) and SARS-CoV-2 pseudovirus (IC_{50} = 80 nM). In both cases, conjugating the peptides with cholesterol enhanced the antiviral effects and HR1 binding stability (107, 109). This cholesterol-modifying strategy has also been used in HIV inhibitors (110, 111).

5.3. Targeting the Main Protease

The main protease, M^{pro}, or 3C-like protease ($3CL^{pro}$) (112), is a 33.8-kDa cysteine protease that mediates viral replication and transcription (113). M^{pro} is highly conserved among all the coronaviruses, especially the substrate-binding site and the active site Cys145–His41 catalytic dyad (22, 114–118). The two polyproteins pp1a and pp1ab are cleaved by papain-like protease (PL^{pro}) and M^{pro} into 16 nonstructural proteins (NSPs), which are essential for envelope, membrane, Spike (S), and nucleocapsid protein production (119, 120). The absence of a human homolog and the availability of the apo structure (PDB ID: 6Y2E) as a template make M^{pro} an attractive target for antiviral drug design (23, 115, 116, 121, 122) (**Figures 2b**, **subpanel i** and **3b**).

In 2020, Dai et al. (21) designed and developed two structure-based anti-SARS-CoV-2 compounds that target M^{pro}: 11a and 11b. The X-ray crystal structures of SARS-CoV-2 M^{pro} in complex with 11a (PDB ID: 6LZE) and 11b (PDB ID: 6M0K) were determined at a resolution of 1.5 Å. Although their chemical structures were different—a cyclohexyl group for 11a versus a 3-fluorophenyl group for 11b—the compounds demonstrated a similar inhibitory mechanism: They occupy the substrate-binding pocket and the aldehyde group of the compounds covalently binds to the catalytic site Cys145 and blocks enzymatic activity of M^{pro} (21). Compounds 11a and 11b display high SARS-CoV-2 M^{pro} inhibitory activity (IC_{50} values = 53 and 40 nM, respectively) (21). The high selectivity indices for 11a (SI > 189) and 11b (SI > 139) indicate that these compounds offer good antiviral activity without significant cytotoxic effects.

N3, a Michael acceptor inhibitor, was previously shown to strongly inhibit SARS-CoV, MERS-CoV, and infectious bronchitis virus in animal models (115). In 2020, Jin et al. (22) solved the crystal structure of N3 in complex with SARS-CoV-2 M^{pro} at resolutions of 2.16 and 1.7 Å (PDB

IDs: 6LU7, 7BQY). N3 binds irreversibly in the M^{pro} substrate recognition pocket and inhibits SARS-CoV-2 with an EC_{50} value of 16 μM.

Two other drugs affect M^{pro}: ebselen and carmofur. These drugs were identified as potential drugs against SARS-CoV-2 through high-throughput screening (22). Ebselen has been studied in clinical trials for noise-induced hearing loss and bipolar disease (123–125), and carmofur is approved in some countries for adjuvant chemotherapy of colorectal cancer and is used clinically to treat breast, gastric, and bladder cancers (126–129). Tandem mass spectrometry analysis revealed that ebselen and carmofur covalently bind to the catalytic Cys145 of SARS-CoV-2 M^{pro}. Carmofur completely modifies M^{pro}, whereas ebselen only partially modifies it. Ebselen shows better inhibition than carmofur ($IC_{50} = 0.67$ versus 1.82 μM), suggesting it may inhibit M^{pro} through noncovalent binding (22), and has a high inhibition efficiency against SARS-CoV-2 ($EC_{50} = 4.67$ μM). These results suggest that ebselen is a potential therapeutic drug for the treatment of COVID-19.

Given that SARS-CoV-2 mainly affects the lungs, studies have sought to explore drugs that are specifically suitable for inhalation. For example, the α-ketoamide 13b inhibitor has been optimized from α-ketoamide 11r, a previously designed drug with picomolar inhibitory activity against MERS-CoV in vitro (130), half-life enhancement in plasma, pronounced lung tropism, and is suitable to be administered by inhalation (23). Zhang and colleagues (23) solved the X-ray crystal structure of SARS-CoV-2 M^{pro} in complex with α-ketoamide 13b at resolutions of 1.95 and 2.20 Å (PDB IDs: 6Y2F, 6Y2G). The α-ketoamide 13b warhead interacts with the catalytic substrate-binding site of SARS-CoV-2 M^{pro} through two hydrogen bonding interactions, thus blocking the protease ($IC_{50} = 900$ nM; $EC_{50} = 4$–5 μM). Compared with other warheads, such as aldehydes (131) (compound 11a and 11b) and Michael acceptors (132) (compound N3), which only have one hydrogen bonding interaction with Cys145, α-ketoamide 13b has two hydrogen bonds, which help lock the inhibitor in the catalytic site (130). A nebulized form of α-ketoamide 13b was tested in mice and was well tolerated with no adverse effects (23), indicating that this drug can be administered by inhalation.

5.4. Targeting Viral Replication

The viral replication machinery, RNA-dependent RNA polymerase (RdRp), plays a pivotal role in genome replication. Several small-molecule nucleoside analogs that mimic naturally occurring nucleosides have been designed to inhibit viral replication (**Figure 2b**, **subpanel ii**). The RNA-binding site on RdRp and the residues involved in the catalytic site are highly conserved among coronaviruses (133, 134). RdRp of SARS-CoV-2 shares 99.1% similarity and 96% amino acid sequence identity with SARS-CoV (135). These structural and functional features make RdRp a promising target for broad-spectrum antivirals.

Remdesivir (GS-5734) is a broad-spectrum antiviral drug originally developed for use against Ebola virus (136) by Gilead Sciences Inc. Results from early clinical trials have shown that patients with advanced COVID-19 recover faster when taking remdesivir (137). In May 2020, the FDA approved remdesivir for emergency use against COVID-19 (138). Remdesivir potently stops viral replication activity via RNA chain termination (136, 139). Using cryo-EM, Yin et al. (24) solved the structure of remdesivir in complex with SARS-CoV-2 RdRp, a 50-base template-primer RNA, at 2.5 Å resolution (PDB ID: 7BV2). In this structure, the partial double-stranded RNA template is inserted into the central channel of RdRp, and remdesivir, covalently added to the first replicated base pair, terminates chain elongation (24) (**Figure 3c**).

RNA virus replication is also targeted by the cytidine analog β-D-N^4-hydroxycytidine (NHC), also known as EIDD-1931. NHC has potent antiviral activities against RNA virus replication and the spread of Ebola virus, hepatitis C virus, Marburg virus, Venezuelan equine encephalitis,

influenza, murine hepatitis virus, and MERS-CoV (140–143), as well as against coronaviruses, including hCoV-NL63, SARS-CoV, and MERS-CoV (144–146). NHC inhibits SARS-CoV-2 replication in Vero cells ($IC_{50} = 300$ nM), Calu-3 cells ($IC_{50} = 80$ nM), and primary human airway epithelial cells ($IC_{50} = 140$ nM), with minimal cytotoxicity of $CC_{50} > 10$ μM (135). The inhibitory activity of coronavirus replication by NHC is consistent with an increased viral mutation rate (143, 147), an effect that is not observed with remdesivir. Sequence analysis of MERS-CoV-infected cells treated with NHC revealed that the mutations that occur are mainly A:G and C:U transitions (135). In murine hepatitis virus, Phe480Leu and Val557Leu mutations in RdRp do not confer resistance to NHC, consistent with data showing that NHC exhibits only a low level of resistance with multiple viruses (141, 143, 147). Nucleoside analogs, such as ribavirin and 5-fluorouracil, are ineffective at targeting coronaviruses due to the proofreading function of the viral 3′-5′ exoribonuclease (ExoN) that removes mismatched nucleosides (148, 149). NHC is only minimally affected by the ExoN proofreading function, suggesting that NHC overcomes the proofreading mechanism and inhibits the replication of coronaviruses.

Because NHC has broad antiviral activity against genetically distinct viruses, Toots et al. (142) developed EIDD-2801, an isopropyl ester prodrug of NHC, which has improved oral bioavailability and pharmacokinetics in vivo. EIDD-2801 drives mutagenesis of viral RNA and causes increased codon change frequency, including stop codons. Thus, treatment with EIDD-2801 can reduce viral load in the lungs and improve pulmonary function in SARS-CoV- or MERS-CoV-infected mouse models (135). The high potency of NHC and EIDD-2801 against other coronaviruses and their oral bioavailability warrant further study of these inhibitors to determine their safety, specificity, and efficacy against SARS-CoV-2 infection.

6. CONCLUSION

In this article, we have presented our analysis of the structural basis for SARS-CoV/CoV-2/MERS–receptor interactions and the potential for small-molecule inhibitors as therapeutics. Comparisons of independent and complex structures have indicated the major therapeutic targets are the NTD and RBD of S-glycoprotein of SARS-CoV-2, SARS-CoV, and MERS-CoV. Structural differences in the RBDs, the hACE2 binding loops, and the presence of the furin cleavage site may explain the higher transmissibility of SARS-CoV-2, and these differences could serve as important targets for drug design. Because of their increased expression during infection, high sequence homology (90%) compared with that of SARS-CoV, and lower mutation rate, SARS-CoV-2 nucleocapsid proteins are emerging as convenient vaccine targets (150, 151). Because the antibodies can bind only to cell surface proteins, the size of inhibitor compounds is relatively small, and the inhibitor compounds can target multiple viral pathways, these compounds are attractive molecules for treating COVID-19.

We highlight the relevance of small-molecule compounds that target two essential viral entry pathways: (*a*) the cathepsin B-/L-dependent pathway, where inhibitors can be used to target cathepsin L, the endosomal proton pump, and autophagy; and (*b*) the protease-mediated plasma membrane entry pathway, where inhibitors can be designed to target TMPRSS2, furin, and the formation of the HR-driven, 6-HB complex. Additionally, M^{pro} can be targeted to inhibit viral protein translation, and the inhibition of RNA replication machinery proteins, such as RdRp, can be designed to impede viral replication. Inhibitor compounds serve as templates for the design and optimization of new drugs, and the repurposing of already-approved drugs with proven antiviral efficacy and specificity, thus allowing a faster route to treatment options. The few drugs thus far in clinical trials have shown some efficacy, with the repurposed drug remdesivir, originally developed for use against Ebola virus, paving the way as a lead drug for treating patients with COVID-19.

Other drugs, such as the serine protease inhibitors camostat mesylate and nafamostat mesylate that target TMPRSS2, have exhibited efficacy that might lead to treatment options. Because most of the small-molecule inhibitors seem to target pathways rather than block binding of the virus to the hACE2 receptor, it is worth exploring recently identified antibodies that neutralize SARS-CoV-2 (50, 152) combined with inhibitor compounds as a multifaceted treatment approach against COVID-19. In vitro experimental data and clinical trial results presented thus far suggest that nafamostat mesylate and remdesivir are potential treatment options for patients with COVID-19. In addition to the use of these repurposed drugs for treatment, previous studies suggest the drugs' use as prophylactics. Nafamostat mesylate and remdesivir prevent endoscopic retrograde cholangiopancreatography (153) and MERS-CoV infection (154), respectively. Although these repurposed drugs show potential, it is unclear which inhibitor might practically prevent disease, cure it, or both.

Apart from the conventional strategies directed toward viral proteins, alternative approaches to target the hACE2 receptor and other host cellular proteins may present promising outcomes for therapeutics and prophylactics against COVID-19. Decoy strategies involving the inhalation of modified soluble recombinant hACE2 and engineered inhibitors like hACE2 conjugated with fragment crystallizable (Fc) domains are being explored as options to treat COVID-19 (37, 155). Because the alternative strategies may provide early protection by blocking interaction between SARS-CoV-2 S-glycoprotein and hACE2 wild type, the severe pathophysiological symptoms (acute lung injury, multiorgan failures) that result from cytokine storms and severe proinflammatory responses of COVID-19 might be reduced. Despite the advantages, these alternative options need extensive in vitro and in vivo testing before they can be approved and used to treat patients.

Collectively, this review highlights a structural perspective on virus–receptor interactions and provides an up-to-date assessment of small-molecule compounds that inhibit coronaviruses, mainly SARS-CoV-2. The potential and newly identified compounds need to be extensively studied in animal models and placebo-controlled clinical trials to establish their efficacy and safety profiles against COVID-19. Given that COVID-19 is a newly discovered virus, it is unclear what type of preventive or therapeutic strategy will be most relevant. As such, the quest for alternative prevention or treatment regimens against COVID-19 must continue progressively and dynamically.

Fc: fragment crystallizable

DISCLOSURE STATEMENT

The authors are not aware of any affiliations, memberships, funding, or financial holdings that might be perceived as affecting the objectivity of this review.

ACKNOWLEDGMENTS

LITERATURE CITED

1. Li W, Hulswit RJG, Widjaja I, Raj VS, McBride R, et al. 2017. Identification of sialic acid-binding function for the Middle East respiratory syndrome coronavirus spike glycoprotein. *PNAS* 114(40):E8508–17
2. Wang Q, Zhang Y, Wu L, Niu S, Song C, et al. 2020. Structural and functional basis of SARS-CoV-2 entry by using human ACE2. *Cell* 181(4):894–904.e9

3. Wrapp D, Wang N, Corbett KS, Goldsmith JA, Hsieh C, et al. 2020. Cryo-EM structure of the 2019-nCoV spike in the prefusion conformation. *Science* 367(6483):1260–63

4. Wu K, Li W, Peng G, Li F. 2009. Crystal structure of NL63 respiratory coronavirus receptor-binding domain complexed with its human receptor. *PNAS* 106(47):19970–74

5. Khan S, Siddique R, Shereen MA, Ali A, Liu J, et al. 2020. Emergence of a novel coronavirus, severe acute respiratory syndrome coronavirus 2: biology and therapeutic options. *J. Clin. Microbiol.* 58(5):e00187-20

6. Zhou P, Yang X-L, Wang X-G, Hu B, Zhang L, et al. 2020. A pneumonia outbreak associated with a new coronavirus of probable bat origin. *Nature* 579(7798):270–73

7. Gorbalenya AE, Baker SC, Baric RS, de Groot RJ, Drosten C, et al. 2020. The species *Severe acute respiratory syndrome-related coronavirus*: classifying 2019-nCoV and naming it SARS-CoV-2. *Nat. Microbiol.* 5(4):536–44

8. Bojkova D, McGreig JE, McLaughlin K-M, Masterson SG, Widera M, et al. 2020. SARS-CoV-2 and SARS-CoV differ in their cell tropism and drug sensitivity profiles. bioRxiv 2020.04.03.024257. **https://doi.org/10.1101/2020.04.03.024257**

9. Quinlan BD, Mou H, Zhang L, Guo Y, He W, et al. 2020. The SARS-CoV-2 receptor-binding domain elicits a potent neutralizing response without antibody-dependent enhancement. bioRxiv 2020.04.10.036418. **https://doi.org/10.1101/2020.04.10.036418**

10. Ou X, Liu Y, Lei X, Li P, Mi D, et al. 2020. Characterization of spike glycoprotein of SARS-CoV-2 on virus entry and its immune cross-reactivity with SARS-CoV. *Nat. Commun.* 11(1):1620

11. Li F. 2008. Structural analysis of major species barriers between humans and palm civets for severe acute respiratory syndrome coronavirus infections. *J. Virol.* 82(14):6984–91

12. Walls AC, Park YJ, Tortorici MA, Wall A, McGuire AT, Veesler D. 2020. Structure, function, and antigenicity of the SARS-CoV-2 spike glycoprotein. *Cell* 181(2):281–92.e6

13. Coutard B, Valle C, de Lamballerie X, Canard B, Seidah NG, Decroly E. 2020. The spike glycoprotein of the new coronavirus 2019-nCoV contains a furin-like cleavage site absent in CoV of the same clade. *Antivir. Res.* 176:104742

14. Srinivasan S, Cui H, Gao Z, Liu M, Lu S, et al. 2020. Structural genomics of SARS-COV-2 indicates evolutionary conserved functional regions of viral proteins. *Viruses* 12(4):360

15. Yuan Y, Cao D, Zhang Y, Ma J, Qi J, et al. 2017. Cryo-EM structures of MERS-CoV and SARS-CoV spike glycoproteins reveal the dynamic receptor binding domains. *Nat. Commun.* 8:15092

16. Wang N, Shi X, Jiang L, Zhang S, Wang D, et al. 2013. Structure of MERS-CoV spike receptor-binding domain complexed with human receptor DPP4. *Cell Res.* 23(8):986–93

17. Hofmann H, Pyrc K, van der Hoek L, Geier M, Berkhout B, Pöhlmann S. 2005. Human coronavirus NL63 employs the severe acute respiratory syndrome coronavirus receptor for cellular entry. *PNAS* 102(22):7988–93

18. Lan J, Ge J, Yu J, Shan S, Zhou H, et al. 2020. Structure of the SARS-CoV-2 spike receptor-binding domain bound to the ACE2 receptor. *Nature* 581(7807):215–20

19. Shang J, Ye G, Shi K, Wan Y, Luo C, et al. 2020. Structural basis of receptor recognition by SARS-CoV-2. *Nature* 581:221–24

20. Li F, Li W, Farzan M, Harrison SC. 2005. Structure of SARS coronavirus spike receptor-binding domain complexed with receptor. *J. Clin. Endocrinol. Metab.* 309:1864–68

21. Dai W, Zhang B, Su H, Li J, Zhao Y, et al. 2020. Structure-based design of antiviral drug candidates targeting the SARS-CoV-2 main protease. *Science* 368(6497):1331–35

22. Jin Z, Du X, Xu Y, Deng Y, Liu M, et al. 2020. Structure of M[pro] from SARS-CoV-2 and discovery of its inhibitors. *Nature* 582(7811):289–93

23. Zhang L, Lin D, Sun X, Curth U, Drosten C, et al. 2020. Crystal structure of SARS-CoV-2 main protease provides a basis for design of improved α-ketoamide inhibitors. *Science* 368(6489):409–12

24. Yin W, Mao C, Luan X, Shen D-D, Shen Q, et al. 2020. Structural basis for the inhibition of the RNA-dependent RNA polymerase from SARS-CoV-2 by remdesivir. *Science* 368(6498):1499–504

25. Chou T. 2007. Stochastic entry of enveloped viruses: fusion versus endocytosis. *Biophys. J.* 93(4):1116–23

26. Wang H, Yang P, Liu K, Guo F, Zhang Y, et al. 2008. SARS coronavirus entry into host cells through a novel clathrin- and caveolae-independent endocytic pathway. *Cell Res.* 18(2):290–301

27. Matsuyama S, Nagata N, Shirato K, Kawase M, Takeda M, Taguchi F. 2010. Efficient activation of the severe acute respiratory syndrome coronavirus spike protein by the transmembrane protease TMPRSS2. *J. Virol.* 84(24):12658–64

28. Belouzard S, Chu VC, Whittaker GR. 2009. Activation of the SARS coronavirus spike protein via sequential proteolytic cleavage at two distinct sites. *PNAS* 106(14):5871–76

29. Qian Z, Dominguez SR, Holmes KV. 2013. Role of the spike glycoprotein of human Middle East respiratory syndrome coronavirus (MERS-CoV) in virus entry and syncytia formation. *PLOS ONE* 8(10):e76469

30. Gierer S, Bertram S, Kaup F, Wrensch F, Heurich A, et al. 2013. The spike protein of the emerging *Betacoronavirus* EMC uses a novel coronavirus receptor for entry, can be activated by TMPRSS2, and is targeted by neutralizing antibodies. *J. Virol.* 87(10):5502–11

31. Glowacka I, Bertram S, Müller MA, Allen P, Soilleux E, et al. 2011. Evidence that TMPRSS2 activates the severe acute respiratory syndrome coronavirus spike protein for membrane fusion and reduces viral control by the humoral immune response. *J. Virol.* 85(9):4122–34

32. Iwata-Yoshikawa N, Okamura T, Shimizu Y, Hasegawa H, Takeda M, Nagata N. 2019. TMPRSS2 contributes to virus spread and immunopathology in the airways of murine models after coronavirus infection. *J. Virol.* 93(6):1–15

33. Hoffmann M, Kleine-Weber H, Schroeder S, Krüger N, Herrler T, et al. 2020. SARS-CoV-2 cell entry depends on ACE2 and TMPRSS2 and is blocked by a clinically proven protease inhibitor. *Cell* 181(2):271–80.e8

34. Hoffmann M, Kleine-Weber H, Pöhlmann S. 2020. A multibasic cleavage site in the spike protein of SARS-CoV-2 is essential for infection of human lung cells. *Mol. Cell* 78(4):779–84.e5

35. Follis KE, York J, Nunberg JH. 2006. Furin cleavage of the SARS coronavirus spike glycoprotein enhances cell–cell fusion but does not affect virion entry. *Virology* 350(2):358–69

36. Yuki K, Fujiogi M, Koutsogiannaki S. 2020. COVID-19 pathophysiology: a review. *Clin. Immunol.* 215:108427

37. Jia HP, Look DC, Shi L, Hickey M, Pewe L, et al. 2005. ACE2 receptor expression and severe acute respiratory syndrome coronavirus infection depend on differentiation of human airway epithelia. *J. Virol.* 79(23):14614–21

38. Towler P, Staker B, Prasad SG, Menon S, Tang J, et al. 2004. ACE2 X-ray structures reveal a large hinge-bending motion important for inhibitor binding and catalysis. *J. Biol. Chem.* 279(17):17996–97

39. Du L, Yang Y, Zhou Y, Lu L, Li F, Jiang S. 2017. MERS-CoV spike protein: a key target for antivirals. *Expert Opin. Ther. Targets* 21(2):131–43

40. Wan Y, Shang J, Graham R, Baric RS, Li F. 2020. Receptor recognition by the novel coronavirus from Wuhan: an analysis based on decade-long structural studies of SARS coronavirus. *J. Virol.* 94(7):e00127-20

41. Watanabe Y, Allen JD, Wrapp D, McLellan JS, Crispin M. 2020. Site-specific glycan analysis of the SARS-CoV-2 spike. *Science* 369(6501):330–33

42. Holm L. 2020. DALI and the persistence of protein shape. *Protein Sci.* 29(1):128–40

43. Thompson JD, Higgins DG, Gibson TJ. 1994. CLUSTAL W: improving the sensitivity of progressive multiple sequence alignment through sequence weighting, position-specific gap penalties and weight matrix choice. *Nucleic Acids Res.* 22(22):4673–80

44. Robert X, Gouet P. 2014. Deciphering key features in protein structures with the new ENDscript server. *Nucleic Acids Res.* 42:W320–24

45. Heinig M, Frishman D. 2004. STRIDE: a web server for secondary structure assignment from known atomic coordinates of proteins. *Nucleic Acids Res.* 32:W500–2

46. Gui M, Song W, Zhou H, Xu J, Chen S, et al. 2017. Cryo-electron microscopy structures of the SARS-CoV spike glycoprotein reveal a prerequisite conformational state for receptor binding. *Cell Res.* 27(1):119–29

47. Kirchdoerfer RN, Wang N, Pallesen J, Wrapp D, Turner HL, et al. 2018. Stabilized coronavirus spikes are resistant to conformational changes induced by receptor recognition or proteolysis. *Sci. Rep.* 8(1):15701

48. Ju B, Zhang Q, Ge J, Wang R, Sun J, et al. 2020. Human neutralizing antibodies elicited by SARS-CoV-2 infection. *Nature* 584:115–19

49. Wrapp D, De Vlieger D, Corbett KS, Torres GM, Wang N, et al. 2020. Structural basis for potent neutralization of betacoronaviruses by single-domain camelid antibodies. *Cell* 181:1004–15

50. Wang C, Li W, Drabek D, Okba NMA, van Haperen R, et al. 2020. A human monoclonal antibody blocking SARS-CoV-2 infection. *Nat. Commun.* 11(1):2251

51. Harrison C. 2020. Coronavirus puts drug repurposing on the fast track. *Nat. Biotechnol.* 38(4):379–81

52. Guy RK, DiPaola RS, Romanelli F, Dutch RE. 2020. Rapid repurposing of drugs for COVID-19. *Science* 368(6493):829–30

53. Jakubcová L, Hollỳ J, Varečková E. 2016. The role of fusion activity of influenza A viruses in their biological properties. *Acta Virol.* 60(2):121–35

54. Hamilton BS, Whittaker GR, Daniel S. 2012. Influenza virus-mediated membrane fusion: determinants of hemagglutinin fusogenic activity and experimental approaches for assessing virus fusion. *Viruses* 4(7):1144–68

55. Mair CM, Ludwig K, Herrmann A, Sieben C. 2014. Receptor binding and pH stability—how influenza A virus hemagglutinin affects host-specific virus infection. *Biochim. Biophys. Acta Biomembr.* 1838 (4):1153–68

56. Shen LW, Mao HJ, Wu YL, Tanaka Y, Zhang W. 2017. TMPRSS2: a potential target for treatment of influenza virus and coronavirus infections. *Biochimie* 142:1–10

57. Simmons G, Gosalia DN, Rennekamp AJ, Reeves JD, Diamond SL, Bates P. 2005. Inhibitors of cathepsin L prevent severe acute respiratory syndrome coronavirus entry. *PNAS* 102(33):11876–81

58. Yang N, Shen HM. 2020. Targeting the endocytic pathway and autophagy process as a novel therapeutic strategy in COVID-19. *Int. J. Biol. Sci.* 16(10):1724–31

59. Chen X, Wang K, Xing Y, Tu J, Yang X, et al. 2014. Coronavirus membrane-associated papain-like proteases induce autophagy through interacting with Beclin1 to negatively regulate antiviral innate immunity. *Protein Cell* 5(12):912–27

60. Gassen NC, Niemeyer D, Muth D, Corman VM, Martinelli S, et al. 2019. SKP2 attenuates autophagy through Beclin1-ubiquitination and its inhibition reduces MERS-coronavirus infection. *Nat. Commun.* 10(1):5770

61. Gassen NC, Papies J, Bajaj T, Dethloff F, Emanuel J, et al. 2020. Analysis of SARS-CoV-2-controlled autophagy reveals spermidine, MK-2206, and niclosamide as putative antiviral therapeutics. bioRxiv 2020.04.15.997254. **https://doi.org/10.1101/2020.04.15.997254**

62. Dong X, Levine B. 2013. Autophagy and viruses: adversaries or allies? *J. Innate Immun.* 5(5):480–93

63. Carmona-Gutierrez D, Bauer MA, Zimmermann A, Kainz K, Hofer SJ, et al. 2020. Digesting the crisis: autophagy and coronaviruses. *Microb. Cell* 7(5):119–28

64. Yao X, Ye F, Zhang M, Cui C, Huang B, et al. 2020. In vitro antiviral activity and projection of optimized dosing design of hydroxychloroquine for the treatment of severe acute respiratory syndrome coronavirus 2 (SARS-CoV-2). *Clin. Infect. Dis.* 71(15):732–39

65. Wang M, Cao R, Zhang L, Yang X, Liu J, et al. 2020. Remdesivir and chloroquine effectively inhibit the recently emerged novel coronavirus (2019-nCoV) in vitro. *Cell Res.* 30:269–71

66. Liu J, Cao R, Xu M, Wang X, Zhang H, et al. 2020. Hydroxychloroquine, a less toxic derivative of chloroquine, is effective in inhibiting SARS-CoV-2 infection in vitro. *Cell Discov.* 6:16

67. Vincent MJ, Bergeron E, Benjannet S, Erickson BR, Rollin PE, et al. 2005. Chloroquine is a potent inhibitor of SARS coronavirus infection and spread. *Virol. J.* 2:69

68. Gao J, Tian Z, Yang X. 2020. Breakthrough: Chloroquine phosphate has shown apparent efficacy in treatment of COVID-19 associated pneumonia in clinical studies. *Biosci. Trends* 14(1):72–73

69. Gautret P, Lagier J-C, Parola P, Hoang VT, Meddeb L, et al. 2020. Hydroxychloroquine and azithromycin as a treatment of COVID-19: results of an open-label non-randomized clinical trial. *Int. J. Antimicrob. Agents* 56(1):105949

70. Alhazzani W, Møller MH, Arabi YM, Loeb M, Gong MN, et al. 2020. Surviving Sepsis Campaign: guidelines on the management of critically ill adults with coronavirus disease 2019 (COVID-19). *Intensive Care Med.* 46(5):854–87

71. Dowall SD, Bewley K, Watson RJ, Vasan SS, Ghosh C, et al. 2016. Antiviral screening of multiple compounds against Ebola virus. *Viruses* 8(11):277

72. Elander B, Fellenius E, Leth R, Olbe L, Wallmark B. 1986. Inhibitory action of omeprazole on acid formation in gastric glands and on H$^+$,K$^+$-ATPase isolated from human gastric mucosa. *Scand. J. Gastroenterol.* 21(3):268–72

73. Long J, Wright E, Molesti E, Temperton N, Barclay W. 2015. Antiviral therapies against Ebola and other emerging viral diseases using existing medicines that block virus entry. *F1000Research* 4:30

74. Shin JM, Kim N. 2013. Pharmacokinetics and pharmacodynamics of the proton pump inhibitors. *J. Neurogastroenterol. Motil.* 19(1):25–35

75. Shang J, Wan Y, Luo C, Ye G, Geng Q, et al. 2020. Cell entry mechanisms of SARS-CoV-2. *PNAS* 117(21):11727–34

76. Huang IC, Bosch BJ, Li F, Li W, Kyoung HL, et al. 2006. SARS coronavirus, but not human coronavirus NL63, utilizes cathepsin L to infect ACE2-expressing cells. *J. Biol. Chem.* 281(6):3198–203

77. Hoffmann M, Hofmann-Winkler H, Pöhlmann S. 2018. Priming time: how cellular proteases arm coronavirus spike proteins. In *Activation of Viruses by Host Proteases*, ed. E Böttcher-Friebertshäuser, W Garten, H Klenk, pp. 71–98. Cham, Switz.: Springer

78. Chowdhury SF, Joseph L, Kumar S, Tulsidas SR, Bhat S, et al. 2008. Exploring inhibitor binding at the S′ subsites of cathepsin L. *J. Med. Chem.* 51(5):1361–68

79. Chowdhury SF, Sivaraman J, Wang J, Devanathan G, Lachance P, et al. 2002. Design of noncovalent inhibitors of human cathepsin L. From the 96-residue proregion to optimized tripeptides. *J. Med. Chem.* 45(24):5321–29

80. Shenoy RT, Sivaraman J. 2011. Structural basis for reversible and irreversible inhibition of human cathepsin L by their respective dipeptidyl glyoxal and diazomethylketone inhibitors. *J. Struct. Biol.* 173(1):14–19

81. Shenoy RT, Chowdhury SF, Kumar S, Joseph L, Purisima EO, Sivaraman J. 2009. A combined crystallographic and molecular dynamics study of cathepsin L retro binding inhibitors. *J. Med. Chem.* 52(20):6335–46

82. Eisenberg T, Knauer H, Schauer A, Büttner S, Ruckenstuhl C, et al. 2009. Induction of autophagy by spermidine promotes longevity. *Nat. Cell Biol.* 11(11):1305–14

83. Igarashi K, Kashiwagi K. 2010. Modulation of cellular function by polyamines. *Int. J. Biochem. Cell Biol.* 42(1):39–51

84. Morselli E, Mariño G, Bennetzen MV, Eisenberg T, Megalou E, et al. 2011. Spermidine and resveratrol induce autophagy by distinct pathways converging on the acetylproteome. *J. Cell Biol.* 192(4):615–29

85. Gupta VK, Scheunemann L, Eisenberg T, Mertel S, Bhukel A, et al. 2013. Restoring polyamines protects from age-induced memory impairment in an autophagy-dependent manner. *Nat. Neurosci.* 16(10):1453–60

86. Mounce BC, Olsen ME, Vignuzzi M, Connor JH. 2017. Polyamines and their role in virus infection. *Microbiol. Mol. Biol. Rev.* 81(4):e00029-17

87. Olsen ME, Filone CM, Rozelle D, Mire CE, Agans KN, et al. 2016. Polyamines and hypusination are required for ebolavirus gene expression and replication. *mBio* 7(4):e00882-16

88. Korovina AN, Tunitskaya VL, Khomutov MA, Simonian AR, Khomutov AR, et al. 2012. Biogenic polyamines spermine and spermidine activate RNA polymerase and inhibit RNA helicase of hepatitis C virus. *Biochemistry* 77(10):1172–80

89. Mounce BC, Poirier EZ, Passoni G, Simon-Loriere E, Cesaro T, et al. 2016. Interferon-induced spermidine-spermine acetyltransferase and polyamine depletion restrict Zika and chikungunya viruses. *Cell Host Microbe* 20(2):167–77

90. Wang RC, Wei Y, An Z, Zou Z, Xiao G, et al. 2012. Akt-mediated regulation of autophagy and tumorigenesis through Beclin 1 phosphorylation. *Science* 338(6109):956–59

91. Degtyarev M, De Mazière A, Orr C, Lin J, Lee BB, et al. 2008. Akt inhibition promotes autophagy and sensitizes PTEN-null tumors to lysosomotropic agents. *J. Cell Biol.* 183(1):101–16

92. Jurgeit A, McDowell R, Moese S, Meldrum E, Schwendener R, Greber UF. 2012. Niclosamide is a proton carrier and targets acidic endosomes with broad antiviral effects. *PLOS Pathog.* 8(10):e10002976

93. Jeon S, Ko M, Lee J, Choi I, Byun SY, et al. 2020. Identification of antiviral drug candidates against SARS-CoV-2 from FDA-approved drugs. *Antimicrob. Agents Chemother.* 64(7):e00819-20

94. Ditzel J, Schwartz M. 1967. Worm cure without tears: the effect of niclosamide on *Taeniasis saginata* in man. *Acta Med. Scand.* 182(5):663–64

95. World Health Organization, Stuart MC, Kouimtzi M, Hill SR, eds. 2009. *WHO Model Formulary 2008*. Geneva: World Health Organization

96. Bestle D, Heindl MR, Limburg H, Van Lam van T, Pilgram O, et al. 2020. TMPRSS2 and furin are both essential for proteolytic activation of SARS-CoV-2 in human airway cells. *Life Sci. Alliance* 3(9):e202000786

97. Lu L, Liu Q, Zhu Y, Chan KH, Qin L, et al. 2014. Structure-based discovery of Middle East respiratory syndrome coronavirus fusion inhibitor. *Nat. Commun.* 5:3067

98. Liu S, Xiao G, Chen Y, He Y, Niu J, et al. 2004. Interaction between heptad repeat 1 and 2 regions in spike protein of SARS-associated coronavirus: implications for virus fusogenic mechanism and identification of fusion inhibitors. *Lancet* 363(9413):938–47

99. Bosch BJ, Martina BEE, Van Der Zee R, Lepault J, Haijema BJ, et al. 2004. Severe acute respiratory syndrome coronavirus (SARS-CoV) infection inhibition using spike protein heptad repeat-derived peptides. *PNAS* 101(22):8455–60

100. Gibo J, Ito T, Kawabe K, Hisano T, Inoue M, et al. 2005. Camostat mesilate attenuates pancreatic fibrosis via inhibition of monocytes and pancreatic stellate cells activity. *Lab. Investig.* 85(1):75–89

101. Marotta F, Fesce E, Rezakovic I, De Chui H, Suzuki K, Idéo G. 1994. Nafamostat mesilate on the course of acute pancreatitis. *Int. J. Pancreatol.* 16(1):51–59

102. Hoffmann M, Schroeder S, Kleine-Weber H, Müller MA, Drosten C, Pöhlmann S. 2020. Nafamostat mesylate blocks activation of SARS-CoV-2: new treatment option for COVID-19. *Antimicrob. Agents Chemother.* 64(6):e00754-20

103. Yamamoto M, Matsuyama S, Li X, Takeda M, Kawaguchi Y, et al. 2016. Identification of nafamostat as a potent inhibitor of Middle East respiratory syndrome coronavirus S protein-mediated membrane fusion using the split-protein-based cell-cell fusion assay. *Antimicrob. Agents Chemother.* 60(11):6532–39

104. Zhirnov OP, Matrosovich TY, Matrosovich MN, Klenk H-D. 2011. Aprotinin, a protease inhibitor, suppresses proteolytic activation of pandemic H1N1v influenza virus. *Antivir. Chem. Chemother.* 21(4):169–74

105. Meyer D, Sielaff F, Hammami M, Böttcher-Friebertshäuser E, Garten W, Steinmetzer T. 2013. Identification of the first synthetic inhibitors of the type II transmembrane serine protease TMPRSS2 suitable for inhibition of influenza virus activation. *Biochem. J.* 452(2):331–43

106. Xia S, Yan L, Xu W, Agrawal AS, Algaissi A, et al. 2019. A pan-coronavirus fusion inhibitor targeting the HR1 domain of human coronavirus spike. *Sci. Adv.* 5(4):eaav4580

107. Xia S, Liu M, Wang C, Xu W, Lan Q, et al. 2020. Inhibition of SARS-CoV-2 (previously 2019-nCoV) infection by a highly potent pan-coronavirus fusion inhibitor targeting its spike protein that harbors a high capacity to mediate membrane fusion. *Cell Res.* 30(4):343–55

108. Xia S, Zhu Y, Liu M, Lan Q, Xu W, et al. 2020. Fusion mechanism of 2019-nCoV and fusion inhibitors targeting HR1 domain in spike protein. *Cell. Mol. Immunol.* 17(7):765–67

109. Zhu Y, Yu D, Yan H, Chong H, He Y. 2020. Design of potent membrane fusion inhibitors against SARS-CoV-2, an emerging coronavirus with high fusogenic activity. *J. Virol.* 94(14):e00635-20

110. Zhu Y, Chong H, Yu D, Guo Y, Zhou Y, He Y. 2019. Design and characterization of cholesterylated peptide HIV-1/2 fusion inhibitors with extremely potent and long-lasting antiviral activity. *J. Virol.* 93(11):e02312-18

111. Chong H, Zhu Y, Yu D, He Y. 2018. Structural and functional characterization of membrane fusion inhibitors with extremely potent activity against human immunodeficiency virus type 1 (HIV-1), HIV-2, and simian immunodeficiency virus. *J. Virol.* 92(20):e01088-18

112. Shi J, Sivaraman J, Song J. 2008. Mechanism for controlling the dimer-monomer switch and coupling dimerization to catalysis of the severe acute respiratory syndrome coronavirus 3C-like protease. *J. Virol.* 82(9):4620–29

113. Anand K, Ziebuhr J, Wadhwani P, Mesters JR, Hilgenfeld R. 2003. Coronavirus main proteinase (3CLpro) structure: basis for design of anti-SARS drugs. *Science* 300(5626):1763–67

114. Hegyi A, Ziebuhr J. 2002. Conservation of substrate specificities among coronavirus main proteases. *J. Gen. Virol.* 83(Part 3):595–99

115. Xue X, Yu H, Yang H, Xue F, Wu Z, et al. 2008. Structures of two coronavirus main proteases: implications for substrate binding and antiviral drug design. *J. Virol.* 82(5):2515–27

116. Ren Z, Yan L, Zhang N, Guo Y, Yang C, et al. 2013. The newly emerged SARS-like coronavirus hCoV-EMC also has an "Achilles' heel": current effective inhibitor targeting a 3C-like protease. *Protein Cell* 4(4):248–50

117. Wang F, Chen C, Tan W, Yang K, Yang H. 2016. Structure of main protease from human coronavirus NL63: insights for wide spectrum anti-coronavirus drug design. *Sci. Rep.* 6:22677

118. Lee CC, Kuo CJ, Ko TP, Hsu MF, Tsui YC, et al. 2009. Structural basis of inhibition specificities of 3C and 3C-like proteases by zinc-coordinating and peptidomimetic compounds. *J. Biol. Chem.* 284(12):7646–55

119. Hilgenfeld R. 2014. From SARS to MERS: crystallographic studies on coronaviral proteases enable antiviral drug design. *FEBS J.* 281(18):4085–96

120. Fehr AR, Perlman S. 2015. Coronaviruses: an overview of their replication and pathogenesis. *Methods Mol. Biol.* 1282:1–23

121. Yang H, Xie W, Xue X, Yang K, Ma J, et al. 2005. Design of wide-spectrum inhibitors targeting coronavirus main proteases. *PLOS Biol.* 3(10):e324

122. Anand K, Palm GJ, Mesters JR, Siddell SG, Ziebuhr J, Hilgenfeld R. 2002. Structure of coronavirus main proteinase reveals combination of a chymotrypsin fold with an extra α-helical domain. *EMBO J.* 21(13):3213–24

123. Kil J, Lobarinas E, Spankovich C, Griffiths SK, Antonelli PJ, et al. 2017. Safety and efficacy of ebselen for the prevention of noise-induced hearing loss: a randomised, double-blind, placebo-controlled, phase 2 trial. *Lancet* 390(10098):969–79

124. Masaki C, Sharpley AL, Cooper CM, Godlewska BR, Singh N, et al. 2016. Effects of the potential lithium-mimetic, ebselen, on impulsivity and emotional processing. *Psychopharmacology* 233(14):2655–61

125. Singh N, Halliday AC, Thomas JM, Kuznetsova O, Baldwin R, et al. 2013. A safe lithium mimetic for bipolar disorder. *Nat. Commun.* 4:1332

126. Sakamoto J, Oba K, Matsui T, Kobayashi M. 2006. Efficacy of oral anticancer agents for colorectal cancer. *Dis. Colon Rectum.* 49(10 Suppl.):S82–91

127. Morimoto K, Koh M. 2003. Postoperative adjuvant use of carmofur for early breast cancer. *Osaka City Med. J.* 49(2):77–83

128. Nishio S, Kishimoto T, Maekawa M, Kawakita J, Morikawa Y, et al. 1987. Study on effectiveness of carmofur (Mifurol®) for urogenital carcinoma, especially bladder cancer, as a post-operative adjuvant chemotherapeutic agent. *Hinyokika Kiyo* 33(2):295–303

129. Gröhn P, Heinonen E, Kumpulainen E, Lansimies H, Lantto A, et al. 1990. Oral carmofur in advanced gastrointestinal cancer. *Am. J. Clin. Oncol. Cancer Clin. Trials* 13(6):477–79

130. Zhang L, Lin D, Kusov Y, Nian Y, Ma Q, et al. 2020. α-Ketoamides as broad-spectrum inhibitors of coronavirus and enterovirus replication: structure-based design, synthesis, and activity assessment. *J. Med. Chem.* 63(9):4562–78

131. Zhu L, George S, Schmidt MF, Al-Gharabli SI, Rademann J, Hilgenfeld R. 2011. Peptide aldehyde inhibitors challenge the substrate specificity of the SARS-coronavirus main protease. *Antiviral Res.* 92(2):204–12

132. Tan J, George S, Kusov Y, Perbandt M, Anemüller S, et al. 2013. 3C protease of enterovirus 68: structure-based design of Michael acceptor inhibitors and their broad-spectrum antiviral effects against picornaviruses. *J. Virol.* 87(8):4339–51

133. te Velthuis AJW. 2014. Common and unique features of viral RNA-dependent polymerases. *Cell. Mol. Life Sci.* 71(22):4403–20

134. Venkataraman S, Prasad BVLS, Selvarajan R. 2018. RNA dependent RNA polymerases: insights from structure, function and evolution. *Viruses* 10(2):76

135. Sheahan TP, Sims AC, Zhou S, Graham RL, Pruijssers AJ, et al. 2020. An orally bioavailable broad-spectrum antiviral inhibits SARS-CoV-2 in human airway epithelial cell cultures and multiple coronaviruses in mice. *Sci. Transl. Med.* 12(541):eabb5883

136. Tchesnokov EP, Feng JY, Porter DP, Götte M. 2019. Mechanism of inhibition of Ebola virus RNA-dependent RNA polymerase by remdesivir. *Viruses* 11(4):326

137. NIH (Natl. Inst. Health). 2020. *NIH clinical trial shows remdesivir accelerates recovery from advanced COVID-19*. News Release, Apr. 29. **https://www.nih.gov/news-events/news-releases/nih-clinical-trial-shows-remdesivir-accelerates-recovery-advanced-covid-19**

138. FDA (Food Drug Adm.). 2020. *Coronavirus (COVID-19) update: FDA issues emergency use authorization for potential COVID-19 treatment*. News Release, May 1. **https://www.fda.gov/news-events/press-announcements/coronavirus-covid-19-update-fda-issues-emergency-use-authorization-potential-covid-19-treatment**

139. Gordon CJ, Tchesnokov EP, Woolner E, Perry JK, Feng JY, et al. 2020. Remdesivir is a direct-acting antiviral that inhibits RNA-dependent RNA polymerase from severe acute respiratory syndrome coronavirus 2 with high potency. *J. Biol. Chem.* 295(20):6785–97

140. Reynard O, Nguyen X-N, Alazard-Dany N, Barateau V, Cimarelli A, Volchkov VE. 2015. Identification of a new ribonucleoside inhibitor of Ebola virus replication. *Viruses* 7(12):6233–40

141. Stuyver LJ, Whitaker T, McBrayer TR, Hernandez-Santiago BI, Lostia S, et al. 2003. Ribonucleoside analogue that blocks replication of bovine viral diarrhea and hepatitis C viruses in culture. *Antimicrob. Agents Chemother.* 47(1):244–54

142. Toots M, Yoon J-J, Cox RM, Hart M, Sticher ZM, et al. 2019. Characterization of orally efficacious influenza drug with high resistance barrier in ferrets and human airway epithelia. *Sci. Transl. Med.* 11(515):eaax5866

143. Urakova N, Kuznetsova V, Crossman DK, Sokratian A, Guthrie DB, et al. 2017. β-D-N^4-hydroxycytidine is a potent anti-alphavirus compound that induces a high level of mutations in the viral genome. *J. Virol.* 92(3):e01965-17

144. Pyrc K, Bosch BJ, Berkhout B, Jebbink MF, Dijkman R, et al. 2006. Inhibition of human coronavirus NL63 infection at early stages of the replication cycle. *Antimicrob. Agents Chemother.* 50(6):2000–8

145. Barnard DL, Hubbard VD, Burton J, Smee DF, Morrey JD, et al. 2004. Inhibition of severe acute respiratory syndrome-associated coronavirus (SARSCoV) by calpain inhibitors and β-D-N^4-hydroxycytidine. *Antivir. Chem. Chemother.* 15(1):15–22

146. Agostini ML, Pruijssers AJ, Chappell JD, Gribble J, Lu X, et al. 2019. Small-molecule antiviral β-D-N^4-hydroxycytidine inhibits a proofreading-intact coronavirus with a high genetic barrier to resistance. *J. Virol.* 93(24):e01348-19

147. Yoon JJ, Toots M, Lee S, Lee ME, Ludeke B, et al. 2018. Orally efficacious broad-spectrum ribonucleoside analog inhibitor of influenza and respiratory syncytial viruses. *Antimicrob. Agents Chemother.* 62(8):e00766-18

148. Smith EC, Blanc H, Vignuzzi M, Denison MR. 2014. Coronaviruses lacking exoribonuclease activity are susceptible to lethal mutagenesis: evidence for proofreading and potential therapeutics. *PLOS Pathog.* 10(7):e1004342

149. Ferron F, Subissi L, De Morais ATS, Le NTT, Sevajol M, et al. 2017. Structural and molecular basis of mismatch correction and ribavirin excision from coronavirus RNA. *PNAS* 115(2):E162–71

150. Padron-Regalado E. 2020. Vaccines for SARS-CoV-2: lessons from other coronavirus strains. *Infect. Dis. Ther.* 9(2):255–74

151. Dutta NK, Mazumdar K, Gordy JT. 2020. The nucleocapsid protein of SARS-CoV-2: a target for vaccine development. *J. Virol.* 94(13):e00647-20

152. Jiang S, Hillyer C, Du L. 2020. Neutralizing antibodies against SARS-CoV-2 and other human coronaviruses. *Trends Immunol.* 41(5):355–59

153. Chang JH, Lee IS, Kim HK, Cho YK, Park JM, et al. 2009. Nafamostat for prophylaxis against post-endoscopic retrograde cholangiopancreatography pancreatitis compared with gabexate. *Gut Liver* 3(3):205–10

154. de Wit E, Feldmann F, Cronin J, Jordan R, Okumura A, et al. 2020. Prophylactic and therapeutic remdesivir (GS-5734) treatment in the rhesus macaque model of MERS-CoV infection. *PNAS* 117(12):6771–76

155. Ameratunga R, Lehnert K, Leung E, Comoletti D, Snell R, et al. 2020. Inhaled modified angiotensin converting enzyme 2 (ACE2) as a decoy to mitigate SARS-CoV-2 infection. *N. Z. Med. J.* 133(1515):112–18

156. Wu CJ, Jan JT, Chen CM, Hsieh HP, Hwang DR, et al. 2004. Inhibition of severe acute respiratory syndrome coronavirus replication by niclosamide. *Antimicrob. Agents Chemother.* 48(7):2693–96

157. Kawase M, Shirato K, van der Hoek L, Taguchi F, Matsuyama S. 2012. Simultaneous treatment of human bronchial epithelial cells with serine and cysteine protease inhibitors prevents severe acute respiratory syndrome coronavirus entry. *J. Virol.* 86(12):6537–45

158. Kassell B, Radicevic M, Ansfield MJ, Laskowski M Sr. 1965. The basic trypsin inhibitor of bovine pancreas IV. The linear sequence of the 58 amino acids. *Biochem. Biophys. Res. Commun.* 18:255–58

159. Jin Z, Zhao Y, Sun Y, Zhang B, Wang H, et al. 2020. Structural basis for the inhibition of SARS-CoV-2 main protease by antineoplastic drug carmofur. *Nat. Struct. Mol. Biol.* 27(6):529–32

160. Sheahan TP, Sims AC, Graham RL, Menachery VD, Gralinski LE, et al. 2017. Broad-spectrum antiviral GS-5734 inhibits both epidemic and zoonotic coronaviruses. *Sci. Transl. Med.* 9(396):eaal3653

161. EMA (Eur. Med. Agency). 2020. *Summary on Compassionate Use*. Amsterdam: EMA. **https://www.ema.europa.eu/en/documents/other/summary-compassionate-use-remdesivir-gilead_en.pdf**